Check for updates

Accepted Article

Seasonal changes in hydrology and permafrost degradation control mineral element-bound DOC transport from permafrost soils to streams

Catherine Hirst[1], Elisabeth Mauclet[1], Arthur Monhonval[1], Emeline Tihon[1], Justin Ledman[2], Edward. A.G. Schuur[2], Sophie Opfergelt[1]

[1] Earth and Life Institute, Université catholique de Louvain, Louvain-la-Neuve, Belgium
[2] Center for Ecosystem Science and Society, Northern Arizona University, Flagstaff, AZ, USA

Corresponding author: Catherine Hirst (catherine.hirst@uclouvain.be)

Key Points:

- Headwater streams capture mineral element-bound DOC colloids from permafrost soils during peak flow events (snowmelt and rain)
- The supply of mineral element-bound DOC colloids from soils to river is amplified at sites of extensive permafrost degradation
- Pre-snowmelt soil thaw and more rapid drainage during summer are hydrological changes favouring colloid transport from soil to river

This article has been accepted for publication and undergone full peer review but has not been through the copyediting, typesetting, pagination and proofreading process, which may lead to differences between this version and the Version of Record. Please cite this article as doi: 10.1029/2021GB007105.

This article is protected by copyright. All rights reserved.

Abstract

Mineral elements bind to dissolved organic carbon (DOC) in permafrost soils, and this may contribute to the stabilisation or the degradation of organic carbon along the soil to river continuum. Permafrost thaw enlarges the pool of soil constituents available for soil to river transfer. The unknown is how changes in hydrology upon permafrost degradation affect the connection between soil-derived mineral element-bound DOC and headwater streams. Here, we study Al, Fe, Ca and DOC concentrations in water from a headwater stream at Eight Mile Lake, Alaska, USA (colloidal (0.22 µm–1 kDa) and truly dissolved (< 1 kDa) fractions) and in soil pore waters sampled across a gradient of permafrost degradation at the same location. We target the peak flow to base flow transition to show that there is a narrow window of mineral element-bound DOC colloid transport from soils to streams. We show that during spring thaw and maximum thaw there is an enhanced lateral transfer of mineral element-bound DOC colloids in extensively degraded sites compared to minimally degraded sites. This is explained by a more rapid response of hydrology at peak flow to base flow transition at degraded sites. Our results suggest that ongoing permafrost degradation and the associated response of soils to changing hydrology can be detected by targeting the composition and size of mineral element-DOC associations in soil waters and headwater streams during peak flow-baseflow transitions.

1 Introduction

The permafrost region represents 22 % of the exposed land surface in the Northern Hemisphere (Zhang et al., 1999), of which 24 – 69 % is expected to thaw by 2100 (IPCC 2019). About 1440-1600 Pg C of organic carbon is stored in permafrost (IPCC 2019), and estimates show that ~ 5 % of permafrost soil organic carbon is lost per year by hydrological transport (Plaza et al., 2019), of which a portion can be transferred to the atmosphere as greenhouse gases contributing to the permafrost carbon feedback (Schuur et al., 2015).

Any factor mediating carbon storage and carbon loss along the hydrological continuum in a permafrost landscape is modulating the permafrost carbon feedback. Under conditions of gradual permafrost thaw, the majority of organic carbon can be transported as dissolved organic carbon (DOC) (Dittmar and Katner, 2003) and a number of factors can influence its fate during riverine transport including the binding to mineral elements (i.e., chemical elements resistant to loss on ignition at 950°C (Chao and Sanzolone, 1992) such as aluminium, iron, and calcium (Ingri et al., 2000; Pokrovsky and Schott, 2002; Pokrovsky et al., 2006; Dahlqvist et al., 2007; Stolpe et al.,

This article is protected by copyright. All rights reserved.

Accepted Article

2013)). A portion of DOC is bound to mineral elements and this association spans a range of size fractions, from colloids to low molecular weight nano-sized entities (Pokrovsky and Schott, 2002). Colloids are defined as the particles spanning a size range between 1 µm to 1 nm (Buffle et al., 1998) and practically are quantified by operationally defined size separation: elements transported in the 0.45 µm or 0.22 µm-1 kDa. In Arctic rivers, these colloids are mainly composed of organic-mineral element complexes and inorganic Fe-bearing phases (Pokrovsky and Schott, 2002). The truly dissolved fraction is defined as the low molecular weight entities transported in the less than 1 kDa (~ 1.3 nm) size fraction. In Arctic rivers, the truly dissolved DOC can be transported as lone molecules, or bind to mineral elements, for example Fe-OC low molecular weight complexes (Ilina et al., 2013). Mineral element-bound DOC colloids can retain DOC in soils (Sundman et al., 2014), rivers (Hirst et al., 2017) and estuaries (Herzog et al., 2020) by complexation (Fe-OC complexes) or with minerals providing surface for adsorption (e.g., organic matter binding to the surface of ferrihydrite) (Karlsson and Persson, 2012; Kleber et al., 2015; Rowley et al., 2018). In addition, colloidal mineral element transport can destabilize DOC by promoting non-photo (Page et al., 2013) and photo-mediated (Ward and Cory, 2016) oxidation of permafrost-derived DOC (Bowen et al., 2020), thereby altering the mineral element-bound DOC colloids. The size and composition of mineral element-bound DOC to headwater streams therefore play a role in mediating lateral and vertical riverine organic carbon fluxes and so the question arises: how does soil to river transport at the start of the fluvial continuum govern the initial form of mineral element-bound DOC on which downstream alteration is superimposed?

Mineral element-bound DOC colloids form under specific physico-chemical conditions in soils (e.g., Tipping et al., 2002) and changes in pH, redox and/or metal/DOC ratio, can alter the composition and quantity of soil mineral element-bound DOC available for transfer to rivers (Jansen et al., 2003; Neubauer et al., 2013; Opfergelt et al., 2017; Herndon et al., 2017). In the context of the warming Arctic (IPCC 2019), hydrological pathways are vulnerable to change (Vonk et al., 2019) (for example, water transport through perennial thaw zones (Walvoord et al., 2019) or the formation of water tracks (Evans et al., 2020)) with subsequent effects on soil physico-chemical conditions and the link between mineral elements and DOC in permafrost soils (Fiedler et al., 2004; Lipson et al., 2010; Newman et al., 2015; Pokrovsky et al., 2016; Herndon et al., 2017; Raudina et al., 2017; Patzner et al., 2020). However, we do not have a clear view on how this changing soil hydrology is modulating the input of mineral element-bound DOC from soils to

This article is protected by copyright. All rights reserved.

Accepted Article

rivers. Understanding how mineral element-bound DOC will respond to changing hydrology, in response to permafrost degradation is a needed factor to include in the quantification of DOC loss from permafrost soils (Vonk et al., 2019; Opfergelt, 2020).

Spring thaw and late-summer rain events (referred as peak events in the following) are two key periods for lateral transport of soil constituents to Arctic rivers (Beel et al., 2021). According to the pulse-shunt model (Raymond et al., 2016), the spring snowmelt and summer rain events are the periods when DOC can be flushed directly from soils into Arctic rivers (Rember and Trefry, 2004; Finlay et al., 2006; Raymond et al., 2007; Spencer et al., 2009; Wickland et al., 2012; Mann et al., 2012; Koch et al., 2013; Kutscher et al., 2017) accompanied by high riverine concentrations of mineral elements (Pokrovsky et al., 2010; Bagard et al., 2011; Krickov et al., 2019; Vorobyev et al., 2019). However, what is not known is how the changes in soil hydrology in response to permafrost degradation will modulate the transfer of mineral element-bound DOC during peak events at the soil-river interface. Future predictions suggest that changes in permafrost degradation and hydrology will coincide with peak flow events during understudied hydrological shoulder periods (Shogren et al., 2020). During spring, predicted earlier snowmelt (Stone et al., 2002) may lead to earlier soil thaw (Ollson et al., 2003; Ling et al., 2003) with evidence that such processes are already altering the source and composition of carbon transported to larger rivers (Schwab et al., 2020). During late summer, the predicted increased variability in active layer thickness (ALT) (Peng et a., 2018) and altered soil moisture and water table depths (WTD) (Andresen et al., 2020; Pegoraro et al., 2020), exacerbated by increased rain intensity (IPCC 2019; Douglas et al., 2020) will drive changes in permafrost hydrology. This evidence for changing hydrology motivates our need to target soils with contrasting permafrost conditions (e.g., ALT and soil temperature) and hydrology (soil moisture and WTD) and to understand changing mineral element-bound DOC supply during peak flow events. In addition, during baseflow periods, there is additional time for in-stream processes to alter the soil-derived DOC and mineral element pool (Pokrovsky et al., 2011, 2012; Shirokova et al., 2012; Ilina et al., 2013, 2014; Rose and Cory, 2014; Oleinikova et al., 2017). The impact of in-stream processing on colloid composition will depend on the form of DOC (e.g., mineral element-bound, Bowen et al., 2020) released from soils to stream. This further motivates our need to understand how hydrology modulates the concentration and composition of mineral element-bound DOC transported from soils to the river. To capture the soil mineral

This article is protected by copyright. All rights reserved.

Accepted Article

element-bound DOC response to changing hydrology as a function of stage of permafrost degradation there is a need to target the peak flow-baseflow transitions.

At Eight Mile Lake, Alaska, USA, permafrost degradation has been ongoing for at least 30 years at Gradient site (Osterkamp et al., 2009; Schuur et al., 2009, 2021) resulting in changing active layer thickness, water table depths, and soil moisture content (Osterkamp et al., 2009; Belshe et al., 2012, 2013; Hicks-Pries et al., 2013) which are driving changes in ecosystem respiration (Schuur et al., 2009; Vogel et al., 2009; Lee et al., 2010) and impacting soil pore water dissolved organic carbon content (Zhang et al., 2017). Nonetheless, the role of mineral elements in binding to DOC in these permafrost soils and their transfer to rivers remains poorly investigated. Our overarching goal is to understand the connection between permafrost degradation and mineral element-bound DOC transfer from permafrost soils to rivers. Our hypotheses are that (i) limited periods of changing hydrology, during spring thaw and summer rain events, serve to transfer mineral element bound DOC colloids from soils to stream; (ii) degradation of permafrost soils and the associated changes in hydrology during spring thaw and summer rain affect the form of mineral element-bound DOC (composition and size) transported to rivers. To test these hypotheses, we characterize the colloids composed of Al-bound DOC, Fe-bound DOC and Ca-bound DOC in river waters and soil pore waters along a thaw gradient during two key seasons (snowmelt and a summer rain event).

2 Materials and Methods

2.1 Study area

The catchment where river waters were collected is Panguingue Creek (PC), Alaska, USA (63.87^{o}N; 149.25^{o}W), and the site where soil pore waters, waters perched on the permafrost table and precipitation were collected is Gradient at Eight Mile Lake (EML) catchment located next to PC (63.87^{o}N; 149.25^{o}W) (Figure 1) (Schuur et al., 2009). These catchments share similar characteristics – both are located at ~ 700 m elevation on a gentle (~ 4 degrees), north facing hill slope surrounded by the northern foothills of the Alaskan Range in Interior Alaska. Their geology is composed of Tertiary sedimentary rocks, overlain by gravelly glacial till and aeolian silt including the Pliocene Nenana gravel. The soils contain permafrost within 1 m of the surface, characterised as Gelisols (Soil Survey Staff, 1999). The soil column is subdivided into units, where Unit 1 corresponds to the contemporary active layer that extends from 0 to ~ 60 cm depth and is

This article is protected by copyright. All rights reserved.

Accepted Article

composed of 0 to ~ 10 cm deep organic mat (containing moss and litter, Hutchings et al., 2019), organic rich-soils to ~ 40 cm deep and mineral rich soils below; and Unit 2 corresponds to the post-glacial Pleistocene and early Holocene soils that extend from ~ 60 cm to ~ 120 cm depth and is composed of cryoturbated mineral soils, derived from loess and glacial till (Osterkamp et al., 2009; Hutchings et al., 2019). These catchments lie at the continuous to discontinuous permafrost boundary and soils are near the point of thaw because of their elevation and geographic position (Romanovsky et al., 2007).

Gradient site at EML is a natural gradient in permafrost thaw and thermokarst development. The site is characterised by an area of minimal permafrost degradation with less-disturbed moist acidic tundra where the vegetation is dominated by tussock forming sedge *Eriophorum vaginatum*; an area of moderate permafrost degradation with shallow thermokarst depressions (< 0.5 m deep) that have developed since 1990 and the tussock tundra is dominated by sedges; and an area of extensive permafrost degradation with thermokarst depressions (0.5-1 m) that have developed over at least the past 30 years (Osterkamp et al., 2009), with tussock tundra dominated by shrubs (*Vaccinium uligonosum*) and mosses (*Sphagnum* spp.) (Schuur et al., 2007). The difference in thaw depths across Gradient site results from the redistribution of water into subsided areas which increases soil thermal conductivity and increases ground heat fluxes within depressions (Osterkamp et al., 2007, 2009; Schuur et al., 2009; Belshe et al., 2012,2013). To set up soil sampling sites with contrasted conditions of permafrost degradation, we compared available soil temperature, soil moisture, ALT and WTD data (archived in the Bonanza Creek LTER database, (Opfergelt et al., 2021) between soil profiles from minimal (MIN) and extensive (EXT) permafrost degradation sites at Gradient. In May 2018, the ALT at sites of MIN and EXT degradation was < 10 cm. In August 2019, the ALT at sites of MIN degradation ranged from 55 cm to 68 cm and the ALT at sites of EXT degradation ranged from 48 cm to 96 cm. The organic layer thickness ranged from 20 cm to 40 cm, showing no distinction between MIN and EXT sites. We targeted two shoulder seasons in the Arctic (Shogren et al., 2020): spring thaw (May 2018) and late summer (August-September 2019). Based on the parameters considered (Supporting Information S1, S2, S3), we selected soil profiles with contrasted stages of permafrost degradation, with the minimally degraded profiles at MIN site and the extensively degraded profiles at EXT site.

This article is protected by copyright. All rights reserved.

Accepted Article

2.2 Water sampling

River water samples were collected in 2018 and 2019. In 2018, these samples were collected every day between May 3 and May 12 capturing the conditions prior to river ice break-up (May 3-May 5), during river ice break-up (May 6-May 9), and after river ice break-up when river bank flooding occurred (May 10-May 12). Before river ice break-up, river waters were collected by drilling a hole into the ice with an ice auger and sampling water from underneath the ice using a pre-rinsed plastic container attached to a non-metal pole. After river ice break-up, river waters were collected using a bucket and string. In 2019, river water samples were collected every day at the end of a three week rain event (August 16), a period of intermittent rain (August 21-August 24) and a period with no rain (August 25-September 3) (S.I. Figure 3). The river water discharge (Q) was measured two times after the rain event in August 2019 (21/08/19 and 24/08/19) at Panguingue Creek. The river (8 m wide) was divided into 2 m sections and the stream velocity was measured at three different depths in each section using a FLO-MATE ISO 9001 device, the discharge was calculated for each section (stream-flow velocity x area of section) and the total discharge was determined as the sum of the individual sections. River water discharge was not determined during the river ice-break up and the rain event.

Soil pore waters were collected in May 2018 and August 2019 from three sites of minimal permafrost degradation (MIN A-B-C in 2018, MIN 1-2-3 in 2019) and three sites of extensive degradation (EXT A-B-C in 2018, EXT 1-2-3 in 2019). These sites are within 15 m and uphill of the highly monitored plots where perched waters were collected at Gradient site (Figure 1c; Schuur et al., 2009). The 2018 and 2019 soil profiles lie within 10 m of each other allowing for comparison between years and seasons. In May 2018, soils were sampled to 20 cm depth and subdivided into 5 cm deep soil horizons using a hammer and chisel. In August 2019, soils were sampled to a maximum depth of 120 cm and subdivided into 5 cm-10 cm horizons. Active Layer samples were collected using a hammer and chisel to as deep as possible (up to 45 cm, unless the water table was higher than 45 cm). Below 45 cm depth, active layer and permafrost samples were collected using a steel pipe (diameter 4.5 cm) that was manually hammered into the soil using a sledge hammer (following the method of Palmtag et al., 2015). Care was taken to accout for compaction in active layer soils and in frozen soil compaction was negligible. All soils were stored in zip-lock plastic bags and kept in a cool, dark box immediately after sampling. Soil pore waters were sampled from thawed active layer and thawed permafrost soils within 6 hours of sampling using

This article is protected by copyright. All rights reserved.

Accepted Article

pre-cleaned macro rhizon soil water samplers (length 9 cm, diameter 4.5 mm, porosity 0.2 µm; Eijkelkamp™). The rhizon samplers were attached to acid-washed 50 ml syringes, held under vacuum with wooden sticks, and inserted into soils for ~ 24 hours in cool, dark conditions. The collected soil pore waters were stored in acid-washed (5 % HNO_3, commercial) polypropylene bottles at ~ 8 °C.

Water perched on the permafrost table was collected in August-September 2019 from 30 cm deep boreholes at the highly monitored plots of minimal and extensive permafrost degradation at Gradient site (Figure 1c; Schuur et al., 2009). The boreholes were drained of standing water, left to refill with laterally flowing active layer waters and subsequently sampled into preconditioned 10 L containers using a battery-operated pump. These water samples will be referred as perched waters.

Snow was sampled on May 1 2018 on Gradient site (63º54'75'' N, 149° 05'10'' W) using plastic gloves and zip-lock bags and transferred into acid-washed polypropylene bottles. Rainwater was sampled on August 23 2019 at Gradient (63°52'42''N, 149°15'17'' W) using acid-washed 50 ml centrifuge tubes and acid-washed plastic funnels. Rainwater was transferred into acid-washed polypropylene bottles within 12 hours of rainfall to avoid possible effects of evaporation. Snow and rainwater samples were stored unfiltered and refrigerated immediately at 8 °C.

Temperature, conductivity and pH were measured on river water and perched water samples in the field with a combined temperature, conductivity and pH probe (Hanna Instruments). The electrode was calibrated daily using pH 4 and 7 buffers (NIST) and a 1.41 mS/cm potassium chloride conductivity standard solution (Certipur®). Redox potential was measured in perched waters using a Thermo Scientific Orian Star electrode. Conductivity and pH were measured on soil pore waters in the lab using a pH and conductivity meter (Mettler Toledo Seven Compact Duo S213) with a conductivity electrode (Inlab 715-4 mm) and pH electrode (Inlab micro). River waters and perched waters were filtered within 5 hours of sampling using a Mityvac® hand pump. Samples for major element concentrations were collected by filtration through pre-cleaned 0.22 µm nitrocellulose filters (Millipore®). Samples for DOC were collected using 0.7 µm pre-combusted glass fiber filters (GF/F) (Whatman®). All waters were stored in acid-washed polypropylene bottles and refrigerated immediately at 8°C. Unfiltered river waters underwent an additional size separation to determine the proportion of elements transported as colloids (0.22 µm-1 kDa size fraction) and the portion of elements transported as truly dissolved species (< 1 kDa fraction). Size

This article is protected by copyright. All rights reserved.

Accepted Article

separation was performed using tubular dialysis membranes (Spectrapore 7®) with a molecular weight cut-off size of 1 kDa (~1.3 nm) (Vasyukova et al., 2010; Vasyukova et al., 2012). Before use, the membranes were washed in 2 % HNO_3 and MilliQ® water. The clean membranes were filled with 50 ml of MilliQ® water, sealed with clips (Spectrapore 7®) and stored in MilliQ® in 2 L containers. In the field, a membrane was transferred into an acid-washed 2 L bottle containing unfiltered river water or perched waters. The container was left to equilibrate for 72 hours, and the water that went through the dialysis membrane was collected and is referred to as dialysis water. All membranes were handled using acid-washed pincettes and gloves to minimize contamination. All filtered and dialysis waters were stored in acid-washed polypropylene bottles and refrigerated immediately at ~ 8 ˚C.

2.3 Oxygen and deuterium isotope measurements and water elemental analysis

Oxygen ($\delta^{18}O$) and deuterium (δD) isotope values were determined on river water, perched water and snow samples using Cavity Ring Down Spectroscopy on a Liquid Water Isotope Analyser (L2140-i, Picarro®). Values are normalized between VSLAP and VSMOW and reported in per mil deviation relative to VSMOW. The reproducibility is > 0.6 ‰ for δD and > 0.1 ‰ for $\delta^{18}O$.

Element concentrations, including elements of interest for their interaction with organic carbon (Al, Ca, Fe) and elements required for atmospheric (K) and dilution-corrections (Na), were determined on river waters, soil pore waters, perched waters, snow and rain by inductively-coupled plasma-optical emission spectrometry (ICP-OES; iCAP 6500 Thermo Fisher Scientific). The accuracy on major element concentrations (± 7, 4, 3, 4, 2 % for K, Na, Ca, Al, Fe, respectively) was assessed using the water reference material SLRS-4 (Yeghicheyan et al., 2001) The detection limits for major element concentrations (K, Na, Ca, Al, Fe) are 0.26, 0.43, 0.05, 0.37, and 0.18 mg/L, respectively. DOC concentrations were determined on river waters, soil pore waters, perched waters, snow and rain using high-temperature catalytic oxidation (Shimadzu® TOC-VCPH) with a detection limit of 0.1 mg/L and accuracy of ± 2 %. Filtration and dialysis membrane major element and DOC blanks were below the respective analytical detection limits. Anion concentrations (SO_4^{2-}, Cl^-, NO_3^-) were determined on river waters, perched waters, snow and rain using an IC20 ion chromatograph (Dionex®) with a detection limit of 0.48, 0.47 and 0.68 mg/L, respectively. The accuracy for SO_4^{2-}, Cl^-, NO_3^- (± 3, 4, 4 % respectively) was assessed using river water certified reference material LGC6025 (UKAS, 2014), with a precision of ± 2 % for each

This article is protected by copyright. All rights reserved.

Accepted Article

anion. Alkalinity was measured on river waters within two weeks of sampling using an automatic titrator (Metrohm 916 Ti-Touch) by titrating over the pH range 4.2 to 4.5 with 0.0025 M HCl.

To calculate the proportion of mineral elements and DOC transported in the colloidal fraction, the element concentrations in the dialysis water (DW, < 1 kDa fraction) are subtracted from the element concentrations in filtered waters (FW, <0.22 µm or 0.7µm), according to the following equations:

Colloidal element fraction (0.22 µm–1 kDa) = FW (< 0.22 µm) – DW (< 1 kDa) Eq. 1

Colloidal DOC fraction (0.7 µm-1 kDa) = FW (< 0.7 µm) – DW (< 1 kDa) Eq. 2

and the proportion of mineral elements or DOC in the colloidal fraction is (FW-DW/ FW)*100. The reliability of the dialysis method was tested by comparing anion concentrations in the dialysis water and in the external dialysis solution. The concentrations of SO_4^{2-} differ by 10 % to 40 % (n = 6) and concentrations of Cl^-, F^-, NO_3^- differ by < 5 % (n = 6) for river waters, suggesting that membrane charge effects do not alter the exchange of mineral elements and organic carbon through the dialysis membrane. To validate the use of dialysis membrane separation on unfiltered waters and ensure consistency with previous studies (Vasyukova et al., 2012; Hirst et al., 2017), dialysis was performed on unfiltered waters and waters filtered at 0.22 µm for one sample (PCHWY 24/08/19 R11). In this sample, the contribution of the < 1 kDa fraction to the unfiltered river water and to the 0.22 µm filtered river water were respectively, 29 and 34 % for DOC, 1.0 and 1.2 % for Fe, and 25 and 30 % for Al, and there is < 6 % difference between the contribution of < 1 kDa fraction to unfiltered and 0.22 µm filtered waters for Ca, Na, K.

To correct for atmospheric input from snow and rain, we identified an element mainly supplied by these sources. Snow contributes 2-8 % of DOC, 6-30 % of Al, 4-28 % of Fe, 0.1-1 % of Ca, and 1-8 % of Na to non-dilution corrected river concentrations, and rain contributes 20-56 % of the DOC, 4-25 % of Al, 0.6-3 % of Fe, 0.4-2 % of Ca and 1-5 % of Na non-dilution corrected river concentrations (Opfergelt et al., 2021). We identified that 30 %-90 % of K is supplied from rain to river water, likely derived from aerosols released during local forest fires in Alaska (Polissar et al., 1998) that were prevalent in Interior Alaska in August 2019 (https://modis.gsfc.nasa.gov/gallery/individual.php?db_date=2019-07-11). This is why we use the

This article is protected by copyright. All rights reserved.

Accepted Article

K concentrations in rainwater to correct river water DOC and mineral element concentrations (https://www.lter.uaf.edu/data) for atmospheric inputs with the equation:

$$[i]^*_{riv} = [i]_{riv} - [K]_{riv} * (i / K)_{precip} \quad \text{Eq. 3}$$

where $[i]^*_{riv}$ is the precipitation-corrected concentration for solute i in stream water (µg/L), $[K]_{riv}$ is the measured concentration of K in stream water (µg/L) and $(i / K)_{precip}$ is the molar ratio of solute i to K in precipitation. The atmospheric contribution was < 5 % for Al, Fe, Ca, Na.

To correct for dilution from snow and rain, Na-normalised element ratios ([X]/[Na]) were used to correct river water element concentrations (previously corrected for atmospheric input with Eq. 3). Sodium is used as the normalising element because conductivity shows a positive correlation with Na concentrations in river and groundwaters (R^2= 0.82, $p < 0.05$), indicating that Na concentrations are governed by dilution.

2.4 Geochemical modeling

The geochemical modelling program Visual MINTEQ (Gustafsson, 2011, version 3.1, October 2014) in conjunction with the Stockholm Humic Model (SHM) was used to estimate the complexation of DOC with mineral elements in the colloidal fraction in Panguingue Creek during May 2018 and August-September 2019. In this model, a proportion of the total DOC is considered as 'active' DOC that is available to bind with protons and metals. The 'active' DOM/ DOC ratio was set to 1.6 and the % of DOC that is fulvic acids was set to 65 %, consistent with Swedish stream waters (Sjostedt et al., 2010). The measured field parameters (pH, water temperature, conductivity, and alkalinity), anion and cation concentrations were used as input values for each river water sample, including the < 1 kDa fraction. Fe was input as Fe(III) and was allowed to precipitate as a 'possible solid' in the river waters, when exceeding the solubility product of ferrihydrite ($Fe(OH)_3$). The output from this modeling allows us to determine the percentage of Al, Ca and Fe transported as i) inorganic dissolved, ii) colloidal mineral element-bound complexes with DOC and iii) colloidal mineral element precipitates in river waters.

2.5 Statistical analysis and data storage

This article is protected by copyright. All rights reserved.

Accepted Article

The difference between measured field parameters, mineral element and DOC concentrations in soil pore waters and perched waters from sites of minimal and extensive degradation were tested using Welch's t-test because of the unequal variance in dataset. The results from these statistical tests are shown in S.I. Table 1, and summarized below. The measured field parameters, oxygen and deuterium isotopes, and elemental concentrations in river waters, soil pore waters and perched waters are stored in the Bonanza Creek LTER database (Opfergelt et al., 2021).

3 Results

3.1 Field parameters on river waters, soil pore waters and perched waters

Between May 3 and May 5 2018, river ice thickness decreased from 93 cm to 84 cm corresponding with an increase in flowing water levels from 5 cm to 28 cm (Figure 2a). River water conductivity decreased steeply between May 3 and May 4 coinciding with decreasing alkalinity, increasing river water temperatures and constant high pH values ranging from 8.1 to 8.2. Between May 6 and May 9 2018, river waters started to flow over the river ice surface, and river water conductivity decreased to 91 µS/cm, pH values decreased to 7.9 and river water temperatures fluctuated between 7.8 ºC and 3.5 ºC, corresponding with increased river water levels. Between May 10 and May 11 2018, blocks of ice floated in the river and river levels increased to the point of overbank flooding. Conductivity values decreased to 39 µS/cm, pH values decreased to 7.0 and alkalinity values decreased to 1.09 meq/L. On May 12, there were no blocks of ice remaining in the river, riverbank flooding had subsided and river water pH increased to 7.3 (Figure 2a).

On August 16 2019, Panguingue Creek was sampled at the end of a three week-long rain event that began on July 12 2019 and ended on August 17 2019 with a cumulative precipitation of 288 mm (Opfergelt et al., 2021, S.I. Figure 3). At the end of the rain event on August 16 2019, corresponding to the time of maximum active layer thaw, river levels were comparable to those observed during spring flooding on May 10-May 11 2018. Between August 17 and September 3, river water levels decreased corresponding with an increase in river water conductivity, alkalinity and pH (Figure 2a). There was intermittent rainfall between August 21-August 24, but river water levels continued to decrease during this time (discharge on August 21: 0.95 m^3/sec; discharge on August 24: 0.78 m^3/sec) showing that brief periods of rain did not perturb the overall trend towards low discharge in Panguingue Creek after the rain event.

This article is protected by copyright. All rights reserved.

Accepted Article

In soil pore waters, between May 3-May 12 2018, the average conductivity (39 ± 9 µS/cm) was lower at MIN compared to EXT sites (52 ± 14 µS/cm). On average pH values were higher at MIN sites (4.8 ± 0.1; n = 3), compared to EXT site (4.4 ± 0.1; n = 3). In May 3 – May 12 2018, there was no increase or decrease in conductivity and pH with depth in the profiles in the 0-20 cm of soil. Between August 16-September 3 2019, the pH in soil pore waters increased with depth at MIN and EXT sites, from an average of 4.9±1.0 in the active layer to 7.0 ± 0.7 in the permafrost (n = 6). The conductivity of soil pore waters increased with depth at both soil sites from an average of 51 ± 27 µS/cm (n = 41) in the active layer to 144 ± 109 µS/cm (n = 16) in the permafrost, with significantly higher values in the permafrost compared to active layer ($p < 0.001$) (Opfergelt et al., 2021).

In perched waters, at MIN site, the pH decreased from 4.3 to 4.1 in August after the rain event, and then increased to 4.5 on September 2, whereas pH values ranged from 4.0 to 4.3 with no change overtime at EXT borehole site. The redox potential in MIN borehole site ranged from 231 mV to 257 mV in August after the rain event and decreased to 194 mV on September 2, compared to values from 230 mV to 258 mV at EXT borehole site (Opfergelt et al., 2021).

3.2 **Oxygen and deuterium isotopes in river waters and perched waters**

$\delta^{18}O$ and δD values in snow, river water and perched waters fell on a local meteoric water line: $\delta D = 7.8\ \delta^{18}O + 2.9$ with the lowest $\delta^{18}O$ and δD values in May 2018 and highest $\delta^{18}O$ and δD values during summer months (Figure 3). In river waters collected in May 2018, $\delta^{18}O$ and δD values were highest before river ice-break up ($\delta^{18}O$ = -19.2 ‰; δD = -148.1) and during snowmelt ($\delta^{18}O$ = -18.7 ‰, δD = -142.5 ‰) and lowest during the period of flooding after river ice break-up ($\delta^{18}O$ = -19.8 ‰; δD = - 151.4 ‰) (Figure 2a, Figure 3). In August-September 2019, $\delta^{18}O$ and δD values in river waters were highest at the end of the rain event on 16 August ($\delta^{18}O$ = -14.5 ‰; δD = -110.0 ‰) and lowest during baseflow conditions on 3 September ($\delta^{18}O$ = -14.5 ‰; δD = -137.3) (Figure 2a). Perched water $\delta^{18}O$ and δD values collected in August-September 2019 were higher than river water values. $\delta^{18}O$ and δD values in perched waters at EXT sites were highest after the rain event (17 August-19 August) and decrease to within the range of values in river water from Panguingue Creek during intermittent rain and summer baseflow conditions (August 20-September 3). In contrast, perched waters at MIN sites showed a narrow range of values (δD = -

This article is protected by copyright. All rights reserved.

Accepted Article

111 ‰ to -115 ‰) throughout the period with δD values and remained similar to values at Panguingue Creek following the rain event (Figure 3).

3.3 **River water elemental composition**

In May 2018, riverine DOC/Na, Al/Na and Fe/Na ratios, used to correct for dilution from snow (section 2.3), increased during snowmelt, with peak for DOC and Al on May 11 at the end of snowmelt and peak for Fe on May 12. In contrast, dilution-corrected Ca/Na ratios increased during snowmelt and river ice break-up, decreased between May 10 and May 11 during initial bank flooding and increased again between May 11 and May 12 coinciding with surface soil exposure in the catchment. In August-September 2019, dilution-corrected DOC/Na, Fe/Na and Al/Na ratios were highest on August 16 and decreased sharply between the rain event on August 16 and August 20. These ratios then gradually decreased between August 20 and September 3 and there is no change in element concentration during intermittent rain (Figure 2b). In contrast, dilution-corrected Ca/Na ratios were lowest on August 16 during the rain event and increased between August 16 and September 3, with no response to intermittent rain (Figure 2b).

3.4 **Soil pore water and perched water elemental composition**

In May 2018, soils were sampled to a depth of 20 cm. In soil pore waters from May 2018, the mean DOC concentrations in the 0-20 cm of soil ranged from 43-92 mg/L with MIN and EXT sites showing similar average concentrations (Figure 4a; $p > 0.5$; S.I. Table 1). The mean Al concentrations ranged from 0.1-0.3 mg/L with EXT sites showing significantly lower average Al concentrations (Figure 4b; $p < 0.1$); the mean Fe concentrations ranged from 0.1-0.5 mg/L where EXT sites showed significantly lower average Fe concentrations compared to MIN sites (Figure 4c; $p < 0.05$) and the mean Ca concentrations ranged from 0.3-1.3 mg/L with MIN and EXT sites showing similar average Ca concentrations (Figure 4d; $p > 0.5$). Considering the change in element concentration with depth, at MIN sites DOC and Ca concentrations were highest in the 0-5 cm waters, whereas Al and Fe concentrations were highest in the 15-20 cm waters for all sites. At EXT sites, there was a 15-30 % decrease in Al and Fe concentrations in the 15-20 cm horizon compared to MIN sites, showing there is a decrease in mineral element concentrations in the extensively degraded soil pore waters during snowmelt.

This article is protected by copyright. All rights reserved.

Accepted Article

In August 2019, soils were sampled to a depth of 120 cm. In soil pore waters from August 2019, the mean DOC concentrations in the active layer ranged from 34.7-97.5 mg/L and DOC was significantly higher at MIN sites compared to EXT sites ($p < 0.001$) (Figure 4e, Figure 5). The mean concentration of Al ranged from 0.5-1.7 mg/L, with no clear distinction between MIN and EXT sites ($p > 0.05$) (Figure 4f); the mean concentration of Fe ranged from 2.0-13.0 with significantly higher Fe concentrations in MIN sites compared to EXT sites ($p < 0.005$) (Figure 4g) and the mean concentration of Ca ranged from 1.5-5.0 mg/L with similar Ca concentrations at MIN and EXT sites ($p > 0.5$) (Figure 4h). Considering the change in element concentration with depth across all sites the active layer is subdivided into an unsaturated horizon (the zone above the water table) and saturated horizon (the zone below the water table). For all sites, DOC concentrations show a significant ($p < 0.05$) increase from the unsaturated (49 ± 10 mg/L, $n = 9$) to the saturated zone (94 ± 13 mg/L, $n = 9$) but no significant increase between the saturated active layer and permafrost (105 ± 47 mg/L, $n = 10$). Aluminium concentrations show a significant ($p < 0.05$) increase between the unsaturated active layer and saturated active layer and then decrease ($p < 0.001$) during the transition between organic-rich saturated active layer, mineral-rich saturated active layer and permafrost ($p < 0.05$), showing that the organic-rich saturated active layer is the zone of Al accumulation at MIN sites. Fe concentrations show a significant increase ($p < 0.001$) between the unsaturated active layer (3.0 ± 0.3 mg/L, $n = 9$) and saturated active layer (13 ± 3 mg/L, $n = 15$), but show a similar range of concentrations in the saturated active layer and permafrost soils. Ca concentrations gradually increase with depth, showing no significantly different concentrations between horizons, but the highest concentrations in the permafrost soils. Element concentrations at EXT sites show several contrasting differences to the sites of minimal degradation in the saturated active layer and permafrost soils. There is a significant decrease in DOC, Al and Fe concentrations in the saturated active layer between MIN sites and EXT sites. In the permafrost soils, Fe and Al concentrations show no significant change in concentrations between the two sites, but DOC and Ca show a decrease ($p < 0.05$) in concentrations at EXT sites compared to MIN sites.

In perched waters from August 2019, DOC and Al concentrations show no significant difference between MIN and EXT sites, whereas average Fe concentrations are higher at MIN sites compared to EXT sites ($p < 0.01$) with the largest difference occurring after the rain event.

This article is protected by copyright. All rights reserved.

Accepted Article

Conversely, Ca concentrations are higher in perched waters at EXT sites ($p < 0.05$) compared to MIN sites with the largest difference occurring during the intermittent rain. At MIN sites, Al and Fe concentrations increase overtime with a larger increase than the analytical uncertainty on the measurement. In contrast, at EXT sites, Al and Fe concentrations remain relatively constant over time in the perched water borehole (Opfergelt et al., 2021).

3.5 Element size distribution and the proportion of DOC-bound elements in river and perched waters

In river waters, during spring thaw, summer rain and summer baseflow, > 90 % of Fe is transported as colloids, with 10 % transported in the truly dissolved fraction in the < 0.22 µm fraction (using the calculation in section 2.3; Figure 2b). In contrast, the proportion of DOC, Al and Ca that are transported as colloids changes in response to the hydrograph. The proportion of colloidal DOC increases from 50 % below the river ice to 60 % during snowmelt and 90 % after snowmelt; and the proportion of colloidal DOC decreases from 90 % during summer rain event to 60 % at summer baseflow conditions. Al shows similar behaviour to DOC, with a high percentage of Al transported as colloids during snowmelt and the rain event and a decrease in the contribution of colloidal Al during baseflow conditions. During peak flow periods in 2018 and 2019, > 60 % of Ca is transported as colloids; in contrast 0 - 35 % of Ca is transported as colloids prior to river ice break-up and 20 % Ca during summer baseflow (Figure 2b). Based on geochemical modelling (section 2.4; S.I. Figure 4), there is an increase in the proportion of Al, Ca, Fe-bound DOC between baseflow and flooding. Between May 3 and May 12, the proportion of colloidal Fe-OC and Al-OC complexes increases sharply at the start of snowmelt, whereas the proportion of colloidal Ca-OC complexes increases gradually over this period. Between August 16 and September 3, > 80 % of Al is bound to DOC, irrespective of the hydrograph; 50 % of Fe is bound to DOC during the rain event but this decreases to ~ 30 % during summer baseflow and there is an increased proportion of inorganic Fe-bearing colloids. The proportion of Ca bound to DOC decreases from ~ 25 % during the rain event to < 5 % during baseflow conditions and there is an increased proportion of inorganic dissolved Ca.

In perched soil water at the site, Al, Ca, Fe and DOC are mainly found as colloids (DOC: 80 % - 90 % colloids, Fe: > 90 % colloids, Al: > 80 % colloids, Ca: 65 % - 85 % colloids) from

This article is protected by copyright. All rights reserved.

Accepted Article

rain event to baseflow (Figure 6). There is no difference in element size distribution between MIN and EXT sites. Based on geochemical modelling, we observe a difference in the proportion of colloidal Fe-OC complexes in boreholes at the two sites, with estimates from Visual MINTEQ showing that 100 % of the Fe colloids are bound to organic carbon by complexation in the EXT active layer borehole, whereas a portion of the colloids are composed of Fe oxyhydroxides (ferrihydrite) in the MIN active layer borehole (S.I. Figure 4e). The proportion of ferrihydrite increased from ~ 20 % of the colloidal fraction on August 22 to 40 % of the colloidal fraction on September 2 2019.

4 Discussion

4.1 Hypothesis 1: The connection between mineral element-bound DOC in permafrost soils and a headwater stream

4.1.1 *Winter baseflow to spring thaw*

Before the start of river ice break-up (Stage 1: May 3 to May 5), the ~ 1 m river ice thickness average soil temperatures below 0^{o}C and volumetric soil moisture contents similar to winter values at Gradient site (S.I. Figure 1) suggests that surface flow paths are not active. The below-river ice stream waters are likely an integration of groundwater in the catchment (McNamara et al., 1997). During this first stage, 50 % of DOC is transported in the truly dissolved fraction (< 1 kDa) which is likely composed of low molecular weight organic acids (e.g., acetic acid) (O'Donnell et al., 2012; Wickland et al., 2012) resulting from microbial degradation of DOC in sub-surface waters. The transport of ~ 90 % Al in inorganic form (S.I. Figure 4) alongside the high pH and alkalinity of below river ice waters (Figure 2a) shows that conditions favour the precipitation of inorganic $Al(OH)_{aq}$ rather than complexation with colloidal DOC (Tipping et al., 2002). The ferrihydrite colloids in below-river ice waters, (only a minor portion of total dissolved Fe is available to form mononuclear complexes with LMW < 1 kDa DOC (Vasyukova et al., 2012; Ilina et al., 2013)). formed at the interface between anoxic sub- and supra- permafrost groundwaters and the hyporheic zone during winter months (Pokrovsky and Schott, 2002; Andersson et al., 2006; Ingri et al., 2006; Dahlquist et al., 2007). The transport of Fe and DOC in distinct pools during winter baseflow conditions is consistent with observations from other boreal non-permafrost systems (Lyven et al., 2003; Neubauer et al., 2013; Vasyukova et al., 2010; Bagard et al., 2011). The high Ca concentration in below-ice river waters (32.5 mg/L) were consistent with the highest stream water

This article is protected by copyright. All rights reserved.

Accepted Article

alkalinity values at the end of winter (Figure 2a) indicating that the weathering of carbonate-rich minerals during groundwater transport is supplying Ca to Panguingue Creek catchment during the winter baseflow period (Dahlqvist et al., 2004). The Ca is mainly transported in inorganic form as hydrolysed inorganic complexes (S.I. Figure 4c), though a portion (10 - 40 %) are transported as colloids and this is similar to the range of colloidal Ca transported in river waters during winter baseflow in boreal rivers (Dahlqvist et al., 2004; Pokrovsky et al., 2010). Of the available colloids, < 5 % are bound with DOC (S.I. Figure 4c) suggesting that inorganic Ca-bearing colloids are also transported in the groundwaters.

During river ice break-up and snowmelt (Stage 2: May 6 to May 9) the 5 ‰ decrease in the δD composition of river waters between the start and end of snowmelt is explained by several factors: i) supply of waters from the surface of river ice which is isotopically depleted relative to the river ice and groundwater (Gibson and Prowse, 2002); ii) initial release of snowmelt waters that are isotopically depleted relative to the snowpack (Figure 2a; Streletskiy et al., 2015); iii) snowmelt supply from different snowpacks with different bulk δD values across the catchment (Laudon et al., 2002; AlaAho et al., 2018). During this stage, surface soil temperatures remain below or at the point of thaw and average soil moisture content overlaps values observed between May 3 and May 5 (S.I. Figure 1). The soils can have a freezing point depression (Overduin et al., 2006), so that soil ice thaw can occur below 0^{o}C and the high porosity of the moss/organic mat means that water can likely travel through the top 10 cm of the frozen soil. However, at the measured temperatures, on average snowmelt waters are not percolating into > 10 cm depth of active layer soils and not targeting the mineral-rich horizons (> 20 cm depth, Hutchings et al., 2019) of active layer soils. Therefore, new meltwaters are mainly feeding the headwater stream during this period (Kane et al., 1991; Hinzman et al., 1991). The increase in DOC concentrations and colloidal DOC during snowmelt is consistent with observations across the Arctic (e.g., Cauwet and Sidorov, 1996; Rember and Trefry, 2004; Pokrovsky et al., 2010). The concomitant increase in Al and Fe concentrations and an increasing proportion of mineral element-bound DOC colloids transported in Panguingue Creek during snowmelt is consistent with observations in larger sub-boreal and boreal river waters (Ingri et al., 2006; Andersson et al., 2006; Dahlquist et al., 2007; Bagard et al., 2011; Herzog et al., 2019). The DOC transported during snowmelt is mainly derived from leaching of surface vegetation and plant litter leaching (Neff et al., 2006; Pokrovsky et al., 2015) composed of lignin-rich, young, aromatic DOC (Guo and Macdonald, 2006; Raymond et

This article is protected by copyright. All rights reserved.

Accepted Article

al., 2007; Striegl et al., 2007; Spencer et al., 2008), that has a high affinity for Al, Fe and Ca (Pokrovsky et al., 2006; Riedel et al., 2012). The similarity between the Al and Fe size distribution (Figure 2b), their complexation with organic carbon (S.I. Figure 4) and colloidal Fe/Al ratio ranging from 2 to 5 suggests that Al and Fe are transported together as larger Fe and Al inorganic colloids with organic matter bound to their surface during snowmelt, consistent with observations in larger Arctic rivers (Pokrovsky et al., 2010). These colloids form in the soil litter and topsoil under low pH (Bergren and Mulder 1995; Neubauer et al., 2013) and high DOC/element ratios (Karlsson and Persson, 2010). During snowmelt, 40 % of Ca is bound to DOC which can be attributed to increased contribution from active layer top soils (Andersson et al., 2006; Dahlquist et al., 2007) where it can either be bound to suspended Fe oxyhydroxides (Ingri and Widerlund, 1994) or to OC (Vasyukova et al., 2012; Krickov et al., 2019). The increase contribution of colloidal Ca during snowmelt (Figure 2b) is consistent with previous studies (Ingri and Widerlund 1994; Andersson et al., 2001; Dahlqvist et al., 2005; Ingri et al., 2006; Pokrovsky et al., 2010).

After river ice break-up and snowmelt (Stage 3: May 10 to May 12), the increase in δD composition and decrease in pH from 7.9 to 7.0 in the headwater stream corresponds with an increase in average soil temperatures and increase in average soil moisture content (S.I. Figure 1). This indicates that there is a mixing of snowmelt waters with thawed soil pore waters in the upper soil horizons and a soil pore water signal is transported to the river during this third stage. The decrease in dilution-corrected riverine DOC, Al and Ca concentrations during the period after snowmelt, suggests a decrease in supply of colloidal mineral element-bound DOC complexes from surface litter after the snowmelt period (Pokrovsky et al., 2006). However, dilution-corrected riverine Fe concentrations follow a separate trend to DOC, Al and Ca during the post-snowmelt period (Figure 2b) which is evidence for the separation of different colloidal pools after the snowmelt period. There may be an additional supply of Fe resulting from the biotic or abiotic Fe(III) reduction in the exposed upper active layer soils (Lipson et al., 2010). Reductive dissolution of Fe(III) increases soil pore water pH (Deng and Stumm, 1993) and this may partly explain the increase in river water pH occurring between May 11 and May 12 (Figure 2a).

4.1.2 Rain event to summer baseflow

To investigate when the riverine colloid pool represents a soil-derived colloid pool during the transition from rain event to baseflow, we first establish if there is a common source of colloids

This article is protected by copyright. All rights reserved.

Accepted Article

throughout this period and then assess possible alteration of this colloidal pool during transport. During the rain event-baseflow transition, there are multiple possible sources of DOC-bearing colloid on top of that supplied directly from the soils (Herndon et al., 2015; Opfergelt et al., 2017). These sources include the release of DOC and mineral elements from the degradation of plant material (Pokrovsky et al., 2006) and mineral element-DOC complexation at the redox front between groundwater input and the riparian zone or hyporheic zone (Pokrovsky and Schott, 2002; Ingri et al., 2006, 2018). Importantly, the supply of colloids from soils to rivers is favored throughout this rain event to baseflow transition because Eight Mile Lake catchment is a gently sloping, well-drained site where water ponding depends on local micro topography (Schuur et al., 2009), suggesting that the surface soils remain connected with the headwater streams throughout the summer. Moreover, the soils at Gradient site at EML are characterised by a ~ 30-60 cm thick organic-rich surface horizon (Osterkamp et al., 2009). The WTD varied between 0 cm and 30 cm at both EXT and MIN sites in August 2019 (Opfergelt et al., 2021) and therefore fluctuates within this organic-rich horizon during August 2019 (Hicks-Pries et al., 2013). The high hydraulic conductivity of this horizon allows for rapid transport of waters into headwater streams (Hinzman et al., 1991; Quinton and Marsh, 1998) suggesting that permafrost active layer soils are the dominant source of colloids to Panguingue Creek during the rain and baseflow periods. This is evidence that a portion of soil-derived mineral element-bound DOC (Herndon et al., 2015; Opfergelt et al., 2017) is transferred to rivers throughout the rain-event to baseflow transition.

During the rain event, the increase in average WTD across Gradient site and the similarity between δD values in perched waters andin Panguingue Creek during the rain event (Figure 3), suggest that rain waters feed the perched waters and are then directly flushed into the headwater stream. During the rain event, the similar proportion of Al, Fe, Ca and DOC transported as colloids (0.22 µm-1 kDa) in perched waters and Panguingue Creek (Figure 6) suggests increasing water volume in the soil raises the water table and transfers mineral element-bound DOC colloids along the surface soil horizon into the river (Carey and Woo, 2001b; Kane et al., 2010; Olefeldt and Roulet, 2012). The Fe/Al ratio is similar in the colloidal and LMW < 1 kDa fraction suggesting that both Fe and Al are mainly transported in colloidal form during this peak flow event. There is mixture of larger inorganic Fe-Al bearing colloids and smaller organic Fe-Al-OC bearing colloids consistent with observations in larger Arctic rivers during summer months (Bagard et al., 2011; Pokrovsky et al., 2016). During this narrow window, the Al-OC, Fe-OC and Ca-OC complexes

This article is protected by copyright. All rights reserved.

Accepted Article

that form in the active layer soils are transported to the river. The proportion of material that has faced "alteration along the way" is limited because of the large direct contribution from soils.

After the rain event, the low cumulative rainfall, decrease in river water levels and increasing pH, conductivity and alkalinity in rivers between August 17 to September 3 (Figure 2a) signify a change towards summer/fall baseflow conditions in Panguingue Creek. The decrease in δD values in Panguingue Creek waters points towards a decreased contribution from rainwaters relative to surface waters and increased time for evaporation in the catchment (Streletskiy et al., 2015). Note that under baseflow conditions, local topography keeps some water in the wells at all time since it cannot drain downwards; as such perched waters are not getting flushed as they were during the rain event. The decrease in riverine δD values (Figure 3) and decrease in Al, Fe, Ca and DOC concentrations (Figure 2b) in Panguingue Creek indicates a decrease in the flushing of mineral element bound-DOC colloids from surface soils. The longer residence time of waters in active layer soils during baseflow conditions, allows for more time for colloid alteration during transport (Ilina et al., 2016). The decrease in the size of the DOC, Al and Ca-bearing colloid pools in Panguingue Creek compared to the perched waters (Figure 2b) can be attributed to alteration of colloids during transport so that larger Al-OC and Ca-OC complexes are altered and there is an increased proportion of Al, Ca and OC in the 'truly dissolved' fraction (e.g., Pokrovsky et al., 2016). During the peak flow to baseflow transition, the increase in Fe/Al ratio and Fe/DOC ratios show that more Fe is progressively transported as larger inorganic Fe oxyhydroxide colloids (rather than smaller Fe-OC colloids). The change in the composition of Fe-bearing colloids can be attributed to the degradation of Fe-OC by abiotic (Neaubeur et al., 2015), microbial (Oleinikova et al., 2017a, b, Oleinikova et al., 2019) and light (Page et al., 2013) driven processes resulting in the formation of Fe oxyhydroxides and low molecular weight DOC (e.g., Porcal et al., 2009; Oleinikova et al., 2017a, b), likewise changes in colloidal Ca-OC complexes during transport, result from the breakdown of Ca-OC complexes and the formation of inorganic colloidal (Winderlund and Ingri, 1994) and dissolved phases. During the peak flow – baseflow transition, any pool of mineral element-bound DOC transported unaltered from soils facing permafrost degradation must be disentangled from additional sources and/or the alteration of colloids during transport (beyond the scope of our study). The soil derived-pool must be separated from the pool affected by i) transformation of the soil-derived mineral element-bound DOC colloids (Page et al., 2013; Cory and Ward, 2015), and/or ii) mixing with mineral element-bound DOC supplied by

This article is protected by copyright. All rights reserved.

Accepted Article

groundwater input into the riparian zone and hyporheic zone (Pokrovsky et al., 2016; Ingri et al., 2006, 2018). On top of this soil colloid transformation, the transformed pool will mix with additional sources from groundwater supply to the riparian zone and hyporheic zone in Panguingue Creek (e.g., Ingri et al., 2018). The observed changes to the soil-derived colloids from peak flow to baseflow highlights that to understand the effect of hydrology on the soil-derived colloidal pool the mineral element-bound DOC in headwaters must be compared to that in waters from the active layer.

4.2 Hypothesis 2: Affect of permafrost degradation, and associated changes in hydrology, on the form of mineral element-bound DOC transported from soils to headwater stream

4.2.1 *Winter baseflow to spring thaw*

According to the soil temperature and soil moisture data (S.I. Figure 1) outlined, during snowmelt in May 2018, the soil pore waters at MIN sites remain frozen and so cannot feed DOC and mineral elements to the river. In contrst, at EXT sites, the soil pore waters thaw to 20 cm depth. The upper 0-15 cm of active layer soils at Gradient site are characterised by an organic mat composed of plant material with a pH ranging from 4.3 to 5.0, characteristic of moist, acidic tundra. The 15-20 cm depth generally marks the transition to an organic-rich soil (Schuur et al., 2009; Hicks Pries et al., 2015; Hutchings et al., 2019). It follows that during snowmelt at EXT sites, colloids are transferred from the organic-mat and upper portion of the organic-rich horizon to the river. The low pH of the soil pore waters (4.3 – 4.7) and high DOC concentration favours binding of organic carbon with Fe and Al to form complexes in the surface soils and release of these complexes to Panguingue Creek (Pokrovsky and Schott, 2002). Moreover, the elevated soil temperatures at 40 cm depth (1.11 ^{o}C) on May 12 (Opfergelt et al., 2021), suggest that unfrozen waters in pockets at depth (talik) can also be pushed out by snowmelt, providing an additional pool of mineral element-bound colloids.

In summary, the sequence of events for mineral element-bound DOC mobilisation at spring thaw can be seen as two scenarios depending on the degradation state of permafrost soils (Figure 7a). For poorly degraded soils, surface soils remain frozen during snowmelt, the pulse of DOC is transported from the surface vegetation, and colloidal mineral element-bound DOC associations

This article is protected by copyright. All rights reserved.

Accepted Article

from deeper active layer are not mobilised. For extensively degraded soils, active layer soil temperatures > 0˚C occur during winter months and/or synchronously with snowmelt and mineral elements and DOC are rapidly leached from these layers of unfrozen soil during this peak flow period. In between these end-members from minimal and extensive permafrost degradation, we have a spectrum of situations which when combined can provide a mixture of mineral element-bound DOC associations during the spring flood period (as in May 2018). The river integrates soils that have different conditions of thaw so that the proportion of colloids derived from vegetation leaching, litter leaching and deeper soils from soils is likely to vary.

4.2.2 Rain event to summer baseflow

During the rain event to summer baseflow transition, the significantly lower DOC, Al and Fe concentrations in all soil horizons (Figure 5) at EXT sites relative to MIN sites can be explained by i) a lower production of colloids in the saturated active layer at EXT relative to MIN site, and/or ii) a higher lateral transport of colloids from soils in EXT relative to MIN site.

The lower production of mineral element-bound DOC colloids at EXT sites relative to MIN sites may be driven by differences in the ALT at the two sites (S.I. Figure 2). At Gradient site, EML, the mechanisms controlling soil organic carbon decomposition vary with depth (Hicks-Pries et al., 2013). Soil moisture and soil-moisture related variables (e.g., WTD and precipitation) control the decomposition of soil organic carbon in the 0-20 cm of surface soil and there is an increasing role of heterotrophic respiration of older soil organic carbon in the 15-80 cm of soil profile. Based on this delineation, the significant decrease in DOC concentrations in soil pore waters at depth at EXT sites (Opfergelt et al., 2021) could occur by increased respiration of soil organic carbon and adsorption of DOC onto mineral surfaces in the soil profile at depth. Vogel et al. (2009) observed a larger carbon loss from soils at EXT site attributed to greater ecosystem respiration during the spring, fall and winter. The deeper soil layers showed 100 times greater CO_2 production (Lee et al., 2010), evidence for enhanced respiration at depth at EXT sites. Zhang et al. (2017) showed that there is increased retention of DOC in the 40-60 cm horizon in Gradient site soils, pointing towards increased adsorption of DOC onto mineral surfaces, such as Fe oxyhydroxides, that is consistent with evidence for the retention of DOC in degraded, mineral-rich soils in other permafrost-dominated catchments (Kawahigashi et al., 2004; Prokuishik et al., 2007). Note that these processes of respiration and adsorption could also be occurring during winter

This article is protected by copyright. All rights reserved.

Accepted Article

months in a talik developing between ~ 40 cm depth at EXT soil sites (soil temperature of + 0.10°C at 40 cm depth throughout the winter; https://www.lter.uaf.edu/data). Together, respiration and adsorption, either occurring during winter or summer months, could explain the lower DOC concentrations in soil pore waters at EXT sites compared to MIN sites, thereby limiting the formation of mineral element-bound DOC colloids.

The higher lateral transport of mineral element-bound DOC colloids at EXT sites relative to MIN sites may be driven by differences in hydrology between these sites. We use the perched waters from 0-30 cm depth boreholes to understand the role of WTD on the soil pore water chemistry. The perched water incorporates vertical and lateral transport of soil pore waters and so provides an integration of the chemical composition of waters after the rain event period. In MIN perched water boreholes, the relatively constant ALT (S.I. Figure 2a) and the relatively constant high WTD (S.I. Figure 2c) suggests that the water table remains close to the surface between August 16 and September 3. Moreover, the relatively constant δD values in MIN throughout the rain event to baseflow time series, suggests that perched waters are not draining or evaporating. In contrast, in EXT perched water boreholes, the decreasing WTD at EXT active layer boreholes between August 16 and September 3 (52% decrease; S.I. Figure 2d) and the decrease in δD values over the time series suggest that rainwaters have drained at EXT (Figure 3). Together this supports that waters at MIN sites have a longer soil residence time and pond in the landscape, whereas waters at EXT sites have a shorter soil residence time and more lateral transport of solutes upon drainage. We now investigate how these contrasting hydrological conditions can affect the composition and concentration of the colloidal pool at MIN and EXT sites. In perched waters at MIN sites, a portion of the colloids is composed of ferrihydrite, whereas at EXT sites, all Fe is bound to DOC (S.I. Figure 4e). Under low Fe/DOC ratios in soil pore waters there are sufficient binding sites on the DOC to accommodate the Fe(II) and/or Fe(III) and Fe-OC complexes form. Whereas at Fe/DOC ratios > 0.03 (Jansen et al., 2003), DOC binding sites are filled and a portion of Fe is precipitated as Fe oxyhydroxides e.g., ferrihydrite. In perched waters at MIN sites, the molar Fe/DOC ratio ranges from 0.27 to 0.36 allowing a portion of Fe to precipitate as ferrihydrite (Figure. 8). This proportion increases from 22 to 44 % of colloids between August 22 and September 2 2019 (S.I. Figure 4e). The longer water residence time may drive the soil pore waters at MIN towards more reducing conditions, evidenced by lowering of the redox potential and increasing pH. These conditions promote Fe-bearing mineral dissolution and the supply of more Fe to the perched water.

This article is protected by copyright. All rights reserved.

Accepted Article

This in turn will shift the Fe/DOC ratio to higher values over the rain event to baseflow period, resulting in an increased contribution of ferrihydrite to perched water upon oxidation (Figure 8). The mineral element-bound DOC colloids are formed faster than they can be leached from the soil resulting in the accumulation of colloids in soil pore waters over this period. A portion of this ferrihydrite may directly contribute to the ferrihydrite identified in the Panguingue Creek headwater stream during the rain event to baseflow transition (S.I. Figure 4). This provides evidence for the supply of an un-transformed colloid with a reactive surface on which transformed DOC can attached to in the river column (Hirst et al., 2017). In contrast, at EXT sites, the proportion of colloids remain relatively stable throughout the transition to baseflow conditions (S.I. Figure 4). These colloids are composed of mineral element-bound DOC complexes and inorganic dissolved species (S.I. Figure 4d-f). There is no ferrihydrite since the molar Fe/DOC ratio in perched waters at EXT sites is 0.016 to 0.021 (Figure 8), which is below the threshold for ferrihydrite formation (Nierop et al., 2002; Jansen et al., 2003; Karlsson and Persson, 2010). The water residence time in the saturated active layer at EXT site is shorter than in MIN site, resulting in a lateral transport of solutes with drainage throughout the transition to baseflow conditions. A shorter soil water residence time limits shifts in redox conditions, thereby preventing ferrihydrite formation. Overall, the contrast in hydrology between MIN and EXT sites drives a higher colloid production at MIN site and a higher lateral transport of colloids at EXT site that together result in lower soil pore water concentrations in DOC, Al and Fe at EXT relative to MIN sites.

In summary, the difference between mineral element and DOC concentrations in soil pore waters at the two end-member sites of permafrost degradation can be explained by i) differences in respiration and DOC adsorption between the two sites and ii) differences in the residence time of waters in permafrost soils. For poorly degraded soils, there is a longer residence time of waters in soils after the rain event allowing for the rate of colloid production to exceed the rate of colloid export - resulting in an additional pool of colloids containing Fe oxyhydroxides (ferrihydrite). For extensively degraded soils that face drainage throughout the rain event to baseflow transition (Figure 7b) there is a shorter residence time of waters in soils leading a lateral transport of colloids from soils to rivers. The rate of colloid export equals the rate of colloid production so there is no change in the quantity or composition of the colloidal pool in perched waters between rain event and baseflow.

This article is protected by copyright. All rights reserved.

Accepted Article

4.3 Impact of future changes in the Arctic on mineral element-bound DOC colloid transport from permafrost soils to headwater streams

Snowmelt: In spring, the timing and rate of snowmelt is projected to change (Bintanja & Andry, 2017; Bring et al., 2016). If an earlier snowmelt period is applied to the scenarios presented in Figure 7a, we hypothesize that only a small portion of the active layer soils will have above 0 °C temperatures and the transport of mineral element-bound DOC colloids from surface soil by the hydrologic pulse will be limited. If a longer period of snowmelt is applied to the scenarios presented in Figure 7a, there is a longer period over which mineral element-bound DOC can be shunted into the headwater stream and a higher potential to capture colloids from the thawed upper active layer soils.

Rainfall: In Interior Alaska, precipitation has increased slightly in recent decades and is projected to rise 15-38 % in winter and 10-25 % in summer by the year 2100 relative to 1986-2005 mean (IPCC 2013). Douglas et al. (2020) provide two examples of anomalous summer rain distributions in Interior Alaska and their effect on flooding and permafrost thaw in 2014 and 2016. In 2014, intense rain events but low cumulative precipitation resulted in flooding, high surface runoff and permafrost thaw. If the conditions in summer 2014 are applied to the scenario of Figure 7b, we hypothesize there to be a short pulse of mineral element-bound DOC colloids transported directly from the permafrost soils. This would be followed by a sharp decrease in connectivity between soil pore waters and headwater stream and the supply of an altered colloidal mineral element bound-DOC pool. In 2016, the rain events were smaller and more frequent and dispersed throughout the summer months resulting in less permafrost inundation and less surface flooding. If the conditions in summer 2016 are applied to the scenario of Figure 7b, there is more frequent saturation of the soil column but less capacity to move colloids towards the headwater stream. The longer water residence times in the catchment will allow for accumulation of Fe, increased ferrihydrite precipitation and more time for in-soil and in-stream colloids alteration. Overall, larger and more frequent rain events in headwater streams will lead to increased connectivity between soil pore waters and headwater stream. According to the pulse-shunt model (Raymond et al., 2016) this suggests that mineral element-bound DOC can be transported into higher order tributaries before in-stream DOC transformation.

This article is protected by copyright. All rights reserved.

Accepted Article

Superposition of snowmelt onto early spring soil thaw and talik formation: There is growing evidence that permafrost soils are thawing during time periods when they previously remained frozen (Devoie et al., 2019). For example, suprapermafrost talik formation (Connon et al., 2018) exposes permafrost soils at depth and base-of-snow melt events (Woo, 1986) thaws the surface soils underneath the snow. Here we show that snowmelt is coincidental with talik formation at ~40 cm in EXT soils and early thaw of surface soils at 0-10 cm in EXT soils. When the period of snowmelt is superimposed onto a portion of unfrozen soil, an additional source of mineral element-bound DOC can be shunted into the headwater stream. During the spring flood period, DOC in headwater streams is transferred to large Arctic rivers (Neff et al 2006) suggesting that any additional pool of colloids released from permafrost soils during spring flood will also be carried into larger Arctic river systems (Bagard et al., 2011). Indeed, Schwab et al., 2020 provide evidence for the export of aged DOC in the Mackenzie River basin during the spring flood in June 2018 and attribute this to the transport of DOC from deeper, previously frozen soil horizons.

Thermokarst development: We have demonstrated that the soil pore water colloid composition and concentration is a function of water residence time in the active layer soils. Here we apply this finding to four different stages of permafrost degradation – and hydrological connectivity - evident across the Arctic: i) in minimally degraded permafrost soils (shallow ALT, little WTD fluctuation because there is minimal lateral drainage flow paths; e.g., Minimal site at EML), the pool of colloids can accumulate during summer months and the composition of the colloids can shift in response to changing physio-chemical conditions in the soil pore waters. The relatively thin ALT at maximum thaw means that less unfrozen soil is available for adsorption of colloids onto mineral surfaces; Minimal site is considered as the control site and in the absence of permafrost thaw the hydrological connectivity is governed by seasonal variability; ii) in gradually thawing permafrost soils (increasing ALT over time and fluctuating WTD, e.g., Extensive site at EML), the water residence time is shorter as compared to minimal thaw so that colloids are transported at a faster rate than they can be replaced; in addition, a thicker portion of active layer is unfrozen – including deeper mineral horizons – providing mineral surfaces for interactions with colloids; iii) with abrupt permafrost thaw in low lying topography forming hollows, depressions and subsidence (e.g., West Siberian Lowlands; Loiko et al., 2017), the water residence time is

This article is protected by copyright. All rights reserved.

Accepted Article

shorter than for gradual thaw and colloids are transported immediately from the site of formation so there is insufficient time for changing physico-chemical conditions or interactions between colloids and mineral surfaces; iv) with abrupt permafrost thaw in sloping topography (e.g., Peel Plateau; Littlefair et al., 2017), there is a large flux of particulate and colloidal material from the walls of slumps or thermo erosion gullys (Shakil et al., 2020). In these abrupt thaw sites, colloids are flushed rapidly from the soil site. Following release, the mineral element-bound DOC pool can be altered during transport and/or attachment to new mineral surfaces in the debris tongue of these abrupt thaw sites (Shakil et al., 2020; Beel et al., 2020).

5 Conclusions

We studied the element concentration, element size distribution and the proportion of element associated with DOC in soil pore waters, perched waters and river waters in a permafrost dominated catchment from Alaska during change in hydrology over two shoulder seasons, i.e., spring thaw and late summer rain events. The main conclusions drawn from this study are:

(i) There is a change in the size and composition of Al, Fe and Ca-bound DOC transported from soils to headwater stream during peak flow to baseflow transition. Peak flow events (snowmelt and rain) are the narrow windows during which mineral element-bound DOC colloids are transported directly from permafrost soils to headwater streams.

(ii) In spring thaw, the combined evidence from soil temperature, soil moisture and soil pore water chemistry shows us that, at sites of minimal permafrost degradation, soils at 0-20 cm depth remain below 0^{o}C during snowmelt and mineral element-bound DOC cannot be laterally transferred, whereas at sites of extensive permafrost degradation, the 0-20 cm depth soil is above 0^{o}C during snowmelt allowing for the transport of thaw-derived mineral element-bound DOC associations to the river waters.

(iii) In late summer, at sites of minimal permafrost degradation, the water table depth remains relatively constant from rain event to baseflow. Under these conditions, there is a limited supply of both mineral element-bound DOC (colloidal OC complexes) and inorganic Fe-bearing (Fe oxyhydroxides) colloids from saturated soils to rivers. In contrast, at sites of extensive permafrost

This article is protected by copyright. All rights reserved.

Accepted Article

degradation, soil drainage leads to a decrease in water table depth between rain events and baseflow resulting in the lateral transfer of mineral element-bound DOC (colloidal OC complexes) from saturated soils to rivers.

(iv) The supply of mineral element-bound DOC colloids from soils to rivers is amplified at sites of extensive permafrost degradation. This additional pool can serve to monitor the response of soils to permafrost degradation and requires targeting peak flow to baseflow transition in Arctic rivers.

Transporting organic carbon in different size fractions influences the portion of low molecular weight DOC transported in rivers, a form that is less prone to form mineral element-bound DOC associations. Changing the portion of organic carbon that is mineral-bound will affect the fate of organic carbon along the Arctic river continuum, e.g., the portion buried in river sediment, the portion transported to larger rivers and the portion converted into greenhouse gases.

AcknowledgmentsWe would like to thank Anne Iserentant, Claudine Givron, Elodie Devos and Hélène Dailly from the analytical platform MOCA at UCLouvain. Meghan Taylor is thanked for her valuable contribution to field logistics and sampling, and Simon Malvaux is thanked for his contribution to field sampling in 2019. Magnus Mörth is thanked for the oxygen and deuterium isotope analysis at Stockholm University. The authors acknowledge funding from the European Research Council (ERC) under the European Union's Horizon 2020 research and innovation programme (ERC Starting Grant, WeThaw, grant agreement n°714617) to S.O, and S.O. acknowledges funding from the Fonds National de la Recherche Scientifique (FNRS, Belgium, FC69480). Datasets for this research are available in Opfergelt et al. (2021). The Bonanza Creek LTER website is acknowledged for the Eight Mile Lake data access, with support from the National Science Foundation Long Term Research in Environmental Biology (LTREB Award number: 1754839), the Department of Energy NICCR Program; Department of Energy Terrestrial Ecosystem Processes; the National Science Foundation CAREER Program; the National Parks Inventory and Monitoring Program; the National Science Foundation Bonanza Creek LTER program; the National Science Foundation Office of Polar Programs and the Arctic Natural Sciences Program. References

References

Abbott, B.W., Larouche, J.R., Jones Jr, J.B., Bowden, W.B. and Balser, A.W., 2014. Elevated dissolved organic carbon biodegradability from thawing and collapsing permafrost. *Journal of Geophysical Research: Biogeosciences*, *119*(10), pp.2049-2063.

This article is protected by copyright. All rights reserved.

Accepted Article

Adhikari, D., Sowers, T., Stuckey, J.W., Wang, X., Sparks, D.L. and Yang, Y., 2019. Formation and redox reactivity of ferrihydrite-organic carbon-calcium co-precipitates. *Geochimica et Cosmochimica Acta*, *244*, pp.86-98.

Ala-Aho, P., Soulsby, C., Pokrovsky, O.S., Kirpotin, S.N., Karlsson, J., Serikova, S., Vorobyev, S.N., Manasypov, R.M., Loiko, S. and Tetzlaff, D., 2018. Using stable isotopes to assess surface water source dynamics and hydrological connectivity in a high-latitude wetland and permafrost influenced landscape. *Journal of Hydrology*, *556*, pp.279-293.

Andersson, K., Dahlqvist, R., Turner, D., Stolpe, B., Larsson, T., Ingri, J. and Andersson, P., 2006. Colloidal rare earth elements in a boreal river: changing sources and distributions during the spring flood. *Geochimica et Cosmochimica Acta*, *70*(13), pp.3261-3274.

Andresen, C.G., Lawrence, D.M., Wilson, C.J., McGuire, A.D., Koven, C., Schaefer, K., Jafarov, E., Peng, S., Chen, X., Gouttevin, I. and Burke, E., 2020. Soil moisture and hydrology projections of the permafrost region–a model intercomparison. *The Cryosphere*, *14*(2), pp.445-459.

Assessment, A.C.I., 2005. Arctic climate impact assessment.

Baalousha, M., Vd Kammer, F., Motelica-Heino, M., Baborowski, M., Hofmeister, C. and Le Coustumer, P., 2006. Size-based speciation of natural colloidal particles by flow field flow fractionation, inductively coupled plasma-mass spectroscopy, and transmission electron microscopy/X-ray energy dispersive spectroscopy: Colloids− trace element interaction. *Environmental science & technology*, *40*(7), pp.2156-2162.

Bagard, M.L., Chabaux, F., Pokrovsky, O.S., Viers, J., Prokushkin, A.S., Stille, P., Rihs, S., Schmitt, A.D. and Dupré, B., 2011. Seasonal variability of element fluxes in two Central Siberian rivers draining high latitude permafrost dominated areas. *Geochimica et Cosmochimica Acta*, *75*(12), pp.3335-3357.

Beel, C.R., Heslop, J.K., Orwin, J.F., Pope, M.A., Schevers, A.J., Hung, J.K.Y., Lafrenière, M.J. and Lamoureux, S.F., 2021. Emerging dominance of summer rainfall driving High Arctic terrestrial-aquatic connectivity. *Nature Communications*, *12*(1), pp.1-9.

Belshe, E.F., Schuur, E.A.G., Bolker, B.M. and Bracho, R., 2012. Incorporating spatial heterogeneity created by permafrost thaw into a landscape carbon estimate. *Journal of Geophysical Research: Biogeosciences*, *117*(G1).

Belshe, E.F., Schuur, E.A.G. and Grosse, G., 2013. Quantification of upland thermokarst features with high resolution remote sensing. *Environmental Research Letters*, *8*(3), p.035016.

Berggren, D. and Mulder, J., 1995. The role of organic matter in controlling aluminum solubility in acidic mineral soil horizons. *Geochimica et Cosmochimica Acta*, *59*(20), pp.4167-4180.

This article is protected by copyright. All rights reserved.

Bhattacharyya, A., Schmidt, M.P., Stavitski, E. and Martínez, C.E., 2018. Iron speciation in peats: chemical and spectroscopic evidence for the co-occurrence of ferric and ferrous iron in organic complexes and mineral precipitates. *Organic Geochemistry*, *115*, pp.124-137.

Bintanja, R. and Andry, O., 2017. Towards a rain-dominated Arctic. *Nature Climate Change*, *7*(4), pp.263-267.

Bowen, J.C., Ward, C.P., Kling, G.W. and Cory, R.M., 2020. Arctic amplification of global warming strengthened by sunlight oxidation of permafrost carbon to CO2. *Geophysical Research Letters*, *47*(12), p.e2020GL087085.

Bring, A., Fedorova, I., Dibike, Y., Hinzman, L., Mård, J., Mernild, S.H., Prowse, T., Semenova, O., Stuefer, S.L. and Woo, M.K., 2016. Arctic terrestrial hydrology: A synthesis of processes, regional effects, and research challenges. *Journal of Geophysical Research: Biogeosciences*, *121*(3), pp.621-649.

Buffle, J., Wilkinson, K.J., Stoll, S., Filella, M. and Zhang, J., 1998. A generalized description of aquatic colloidal interactions: the three-colloidal component approach. *Environmental Science & Technology*, *32*(19), pp.2887-2899.

Carey, S.K., 2003. Dissolved organic carbon fluxes in a discontinuous permafrost subarctic alpine catchment. *Permafrost and Periglacial Processes*, *14*(2), pp.161-171.cf

Cauwet, G. and Sidorov, I., 1996. The biogeochemistry of Lena River: organic carbon and nutrients distribution. *Marine Chemistry*, *53*(3-4), pp.211-227.

Chao, T.T. and Sanzolone, R.F., 1992. Decomposition techniques. *Journal of Geochemical Exploration*, *44*(1-3), pp.65-106.

Chen, C., Hall, S.J., Coward, E. and Thompson, A., 2020. Iron-mediated organic matter decomposition in humid soils can counteract protection. *Nature communications*, *11*(1), pp.1-13.

Conrad, S., Ingri, J., Gelting, J., Nordblad, F., Engström, E., Rodushkin, I., Andersson, P.S., Porcelli, D., Gustafsson, Ö., Semiletov, I. and Öhlander, B., 2019. Distribution of Fe isotopes in particles and colloids in the salinity gradient along the Lena River plume, Laptev Sea. *Biogeosciences*, *16*(6).

Cory, R.M., Ward, C.P., Crump, B.C. and Kling, G.W., 2014. Sunlight controls water column processing of carbon in arctic fresh waters. *Science*, *345*(6199), pp.925-928.

Dahlqvist, R., Benedetti, M.F., Andersson, K., Turner, D., Larsson, T., Stolpe, B. and Ingri, J., 2004. Association of calcium with colloidal particles and speciation of calcium in the Kalix and Amazon rivers. *Geochimica et Cosmochimica Acta*, *68*(20), pp.4059-4075.

This article is protected by copyright. All rights reserved.

Dahlqvist, R., Andersson, K., Ingri, J., Larsson, T., Stolpe, B. and Turner, D., 2007. Temporal variations of colloidal carrier phases and associated trace elements in a boreal river. *Geochimica et Cosmochimica Acta*, *71*(22), pp.5339-5354.

Deng, Y. and Stumm, W., 1993. Kinetics of redox cycling of iron coupled with fulvic acid. *Aquatic sciences*, *55*(2), pp.103-111.

Dittmar, T. and Kattner, G., 2003. The biogeochemistry of the river and shelf ecosystem of the Arctic Ocean: a review. *Marine chemistry*, *83*(3-4), pp.103-120.

Douglas, T.A., Turetsky, M.R. and Koven, C.D., 2020. Increased rainfall stimulates permafrost thaw across a variety of Interior Alaskan boreal ecosystems. *npj Climate and Atmospheric Science*, *3*(1), pp.1-7.

Finlay, J., Neff, J., Zimov, S., Davydova, A. and Davydov, S., 2006. Snowmelt dominance of dissolved organic carbon in high- latitude watersheds: Implications for characterization and flux of river DOC. *Geophysical Research Letters*, *33*(10).

Frauenfeld, O.W., Zhang, T., Barry, R.G. and Gilichinsky, D., 2004. Interdecadal changes in seasonal freeze and thaw depths in Russia. *Journal of Geophysical Research: Atmospheres*, *109*(D5).

Frauenfeld, O.W., Zhang, T. and Mccreight, J.L., 2007. Northern hemisphere freezing/thawing index variations over the twentieth century. *International Journal of Climatology: A Journal of the Royal Meteorological Society*, *27*(1), pp.47-63.

Fraysse, F., Pokrovsky, O.S. and Meunier, J.D., 2010. Experimental study of terrestrial plant litter interaction with aqueous solutions. *Geochimica et Cosmochimica Acta*, *74*(1), pp.70-84.

Gibson, J.J. and Prowse, T.D., 2002. Stable isotopes in river ice: Identifying primary over-winter streamflow signals and their hydrological significance. *Hydrological Processes*, *16*(4), pp.873-890.

Guo, L. and Macdonald, R.W., 2006. Source and transport of terrigenous organic matter in the upper Yukon River: Evidence from isotope (δ13C, Δ14C, and δ15N) composition of dissolved, colloidal, and particulate phases. *Global Biogeochemical Cycles*, *20*(2).

Guo, L., Ping, C.L. and Macdonald, R.W., 2007. Mobilization pathways of organic carbon from permafrost to arctic rivers in a changing climate. *Geophysical Research Letters*, *34*(13).

Gustafsson, J.P., 2011. Visual MINTEQ Version 3.1: A Windows version of MINTEQA2.

Herndon, E., AlBashaireh, A., Singer, D., Chowdhury, T.R., Gu, B. and Graham, D., 2017. Influence of iron redox cycling on organo-mineral associations in Arctic tundra soil. *Geochimica et Cosmochimica Acta*, *207*, pp.210-231.

This article is protected by copyright. All rights reserved.

Accepted Article

Herndon, E.M., Yang, Z., Bargar, J., Janot, N., Regier, T.Z., Graham, D.E., Wullschleger, S.D., Gu, B. and Liang, L., 2015. Geochemical drivers of organic matter decomposition in arctic tundra soils. *Biogeochemistry*, *126*(3), pp.397-414.

Herndon, E.M., Mann, B.F., Roy Chowdhury, T., Yang, Z., Wullschleger, S.D., Graham, D., Liang, L. and Gu, B., 2015. Pathways of anaerobic organic matter decomposition in tundra soils from Barrow, Alaska. *Journal of Geophysical Research: Biogeosciences*, *120*(11), pp.2345-2359.

Herzog, S.D., Conrad, S., Ingri, J., Persson, P. and Kritzberg, E.S., 2019. Spring flood induced shifts in Fe speciation and fate at increased salinity. *Applied Geochemistry*, *109*, p.104385.

Herzog, S.D., Persson, P., Kvashnina, K. and Kritzberg, E.S., 2020. Organic iron complexes enhance iron transport capacity along estuarine salinity gradients of Baltic estuaries. *Biogeosciences*, *17*(2), pp.331-344.

Hicks Pries, C.E., van Logtestijn, R.S., Schuur, E.A., Natali, S.M., Cornelissen, J.H., Aerts, R. and Dorrepaal, E., 2015. Decadal warming causes a consistent and persistent shift from heterotrophic to autotrophic respiration in contrasting permafrost ecosystems. *Global change biology*, *21*(12), pp.4508-4519.

Hinkel, K.M. and Nelson, F.E., 2003. Spatial and temporal patterns of active layer thickness at Circumpolar Active Layer Monitoring (CALM) sites in northern Alaska, 1995–2000. *Journal of Geophysical Research: Atmospheres*, *108*(D2).

Hinzman, L.D., Bettez, N.D., Bolton, W.R., Chapin, F.S., Dyurgerov, M.B., Fastie, C.L., Griffith, B., Hollister, R.D., Hope, A., Huntington, H.P. and Jensen, A.M., 2005. Evidence and implications of recent climate change in northern Alaska and other arctic regions. *Climatic change*, *72*(3), pp.251-298.

Hinzman, L.D., Kane, D.L., Gieck, R.E. and Everett, K.R., 1991. Hydrologic and thermal properties of the active layer in the Alaskan Arctic. *Cold Regions Science and Technology*, *19*(2), pp.95-110.

Hirst, C., Andersson, P.S., Shaw, S., Burke, I.T., Kutscher, L., Murphy, M.J., Maximov, T., Pokrovsky, O.S., Mörth, C.M. and Porcelli, D., 2017. Characterisation of Fe-bearing particles and colloids in the Lena River basin, NE Russia. *Geochimica et Cosmochimica Acta*, *213*, pp.553-573.

Holmes, R.M., McClelland, J.W., Peterson, B.J., Tank, S.E., Bulygina, E., Eglinton, T.I., Gordeev, V.V., Gurtovaya, T.Y., Raymond, P.A., Repeta, D.J. and Staples, R., 2012. Seasonal and annual fluxes of nutrients and organic matter from large rivers to the Arctic Ocean and surrounding seas. *Estuaries and Coasts*, *35*(2), pp.369-382.

Hutchings, J.A., Bianchi, T.S., Kaufman, D.S., Kholodov, A.L., Vaughn, D.R. and Schuur, E.A.G., 2019. Millennial-scale carbon accumulation and molecular transformation in a permafrost core from Interior Alaska. *Geochimica et Cosmochimica Acta*, *253*, pp.231-248.

This article is protected by copyright. All rights reserved.

Accepted Article

Ilina, S.M., Poitrasson, F., Lapitskiy, S.A., Alekhin, Y.V., Viers, J. and Pokrovsky, O.S., 2013. Extreme iron isotope fractionation between colloids and particles of boreal and temperate organic-rich waters. *Geochimica et Cosmochimica Acta*, *101*, pp.96-111.

Ilina, S.M., Lapitskiy, S.A., Alekhin, Y.V., Viers, J., Benedetti, M. and Pokrovsky, O.S., 2016. Speciation, size fractionation and transport of trace elements in the continuum soil water–mire–humic lake–river–large oligotrophic lake of a Subarctic watershed. *Aquatic geochemistry*, *22*(1), pp.65-95.

Ingri, J., Widerlund, A., Land, M., Gustafsson, Ö., Andersson, P. and Öhlander, B., 2000. Temporal variations in the fractionation of the rare earth elements in a boreal river; the role of colloidal particles. *Chemical Geology*, *166*(1-2), pp.23-45.

Ingri, J., Malinovsky, D., Rodushkin, I., Baxter, D.C., Widerlund, A., Andersson, P., Gustafsson, Ö., Forsling, W. and Öhlander, B., 2006. Iron isotope fractionation in river colloidal matter. *Earth and Planetary Science Letters*, *245*(3-4), pp.792-798.

Ingri, J. and Widerlund, A., 1994. Uptake of alkali and alkaline-earth elements on suspended iron and manganese in the Kalix River, northern Sweden. *Geochimica et Cosmochimica Acta*, *58*(24), pp.5433-5442.

IPCC 2019 IPCC Special Report on the Ocean and Cryosphere in a Changing Climate, eds H-O Pörtner et al in press

Jager, D.F., Wilmking, M. and Kukkonen, J.V., 2009. The influence of summer seasonal extremes on dissolved organic carbon export from a boreal peatland catchment: Evidence from one dry and one wet growing season. *Science of the Total Environment*, *407*(4), pp.1373-1382.

Jansen, B., Nierop, K.G. and Verstraten, J.M., 2003. Mobility of Fe (II), Fe (III) and Al in acidic forest soils mediated by dissolved organic matter: influence of solution pH and metal/organic carbon ratios. *Geoderma*, *113*(3-4), pp.323-340.

Jorgenson, M.T. and Osterkamp, T.E., 2005. Response of boreal ecosystems to varying modes of permafrost degradation. *Canadian Journal of Forest Research*, *35*(9), pp.2100-2111.

Kane, D.L., Yoshikawa, K. and McNamara, J.P., 2013. Regional groundwater flow in an area mapped as continuous permafrost, NE Alaska (USA). *Hydrogeology Journal*, *21*(1), pp.41-52.

Kane, D.L., Hinzman, L.D., Gieck, R.E., McNamara, J.P., Youcha, E.K. and Oatley, J.A., 2008. Contrasting extreme runoff events in areas of continuous permafrost, Arctic Alaska. *Hydrology Research*, *39*(4), pp.287-298.

Karlsson, T. and Persson, P., 2012. Complexes with aquatic organic matter suppress hydrolysis and precipitation of Fe (III). *Chemical Geology*, *322*, pp.19-27.

This article is protected by copyright. All rights reserved.

Karlsson, T. and Persson, P., 2010. Coordination chemistry and hydrolysis of Fe (III) in a peat humic acid studied by X-ray absorption spectroscopy. *Geochimica et Cosmochimica Acta*, *74*(1), pp.30-40.

Kawahigashi, M., Kaiser, K., Kalbitz, K., Rodionov, A. and Guggenberger, G., 2004. Dissolved organic matter in small streams along a gradient from discontinuous to continuous permafrost. *Global Change Biology*, *10*(9), pp.1576-1586.

Kleber, M., Eusterhues, K., Keiluweit, M., Mikutta, C., Mikutta, R. and Nico, P.S., 2015. Mineral–organic associations: formation, properties, and relevance in soil environments. In *Advances in agronomy* (Vol. 130, pp. 1-140). Academic Press.

Krickov, I.V., Pokrovsky, O.S., Manasypov, R.M., Lim, A.G., Shirokova, L.S. and Viers, J., 2019. Colloidal transport of carbon and metals by western Siberian rivers during different seasons across a permafrost gradient. *Geochimica et Cosmochimica Acta*, *265*, pp.221-241.

Kutscher, L., Mörth, C.M., Porcelli, D., Hirst, C., Maximov, T.C., Petrov, R.E. and Andersson, P.S., 2017. Spatial variation in concentration and sources of organic carbon in the Lena River, Siberia. *Journal of Geophysical Research: Biogeosciences*, *122*(8), pp.1999-2016.

Lamhonwah, D., Lafrenière, M.J., Lamoureux, S.F. and Wolfe, B.B., 2017. Evaluating the hydrological and hydrochemical responses of a High Arctic catchment during an exceptionally warm summer. *Hydrological Processes*, *31*(12), pp.2296-2313.

Laudon, H., Hemond, H.F., Krouse, R. and Bishop, K.H., 2002. Oxygen 18 fractionation during snowmelt: Implications for spring flood hydrograph separation. *Water Resources Research*, *38*(11), pp.40-1.

Lee, H., Schuur, E.A., Vogel, J.G., Lavoie, M., Bhadra, D. and Staudhammer, C.L., 2011. A spatially explicit analysis to extrapolate carbon fluxes in upland tundra where permafrost is thawing. *Global change biology*, *17*(3), pp.1379-1393.

Ling, F. and Zhang, T., 2003. Impact of the timing and duration of seasonal snow cover on the active layer and permafrost in the Alaskan Arctic. *Permafrost and Periglacial Processes*, *14*(2), pp.141-150.

Lipson, D.A., Jha, M., Raab, T.K. and Oechel, W.C., 2010. Reduction of iron (III) and humic substances plays a major role in anaerobic respiration in an Arctic peat soil. *Journal of Geophysical Research: Biogeosciences*, *115*(G4).

Littlefair, C.A., Tank, S.E. and Kokelj, S.V., 2017. Retrogressive thaw slumps temper dissolved organic carbon delivery to streams of the Peel Plateau, NWT, Canada. *Biogeosciences*, *14*(23), pp.5487-5505.

This article is protected by copyright. All rights reserved.

Loiko, S.V., Pokrovsky, O.S., Raudina, T.V., Lim, A., Kolesnichenko, L.G., Shirokova, L.S., Vorobyev, S.N. and Kirpotin, S.N., 2017. Abrupt permafrost collapse enhances organic carbon, CO2, nutrient and metal release into surface waters. *Chemical Geology*, *471*, pp.153-165.

Lyvén, B., Hassellöv, M., Turner, D.R., Haraldsson, C. and Andersson, K., 2003. Competition between iron-and carbon-based colloidal carriers for trace metals in a freshwater assessed using flow field-flow fractionation coupled to ICPMS. *Geochimica et Cosmochimica Acta*, *67*(20), pp.3791-3802

MacLean, R., Oswood, M.W., Irons, J.G. and McDowell, W.H., 1999. The effect of permafrost on stream biogeochemistry: a case study of two streams in the Alaskan (USA) taiga. *Biogeochemistry*, *47*(3), pp.239-267.

Mankin, J.S. and Diffenbaugh, N.S., 2015. Influence of temperature and precipitation variability on near-term snow trends. *Climate Dynamics*, *45*(3-4), pp.1099-1116.

Mann, P.J., Davydova, A., Zimov, N., Spencer, R.G.M., Davydov, S., Bulygina, E., Zimov, S. and Holmes, R.M., 2012. Controls on the composition and lability of dissolved organic matter in Siberia's Kolyma River basin. *Journal of Geophysical Research: Biogeosciences*, *117*(G1).

Mann, P.J., Eglinton, T.I., McIntyre, C.P., Zimov, N., Davydova, A., Vonk, J.E., Holmes, R.M. and Spencer, R.G., 2015. Utilization of ancient permafrost carbon in headwaters of Arctic fluvial networks. *Nature Communications*, *6*(1), pp.1-7.

McNamara, J.P., Kane, D.L. and Hinzman, L.D., 1997. Hydrograph separations in an Arctic watershed using mixing model and graphical techniques. *Water Resources Research*, *33*(7), pp.1707-1719.

Meredith, M., Sommerkorn, M., Cassotta, S., Derksen, C., Ekaykin, A., Hollowed, A., Kofinas, G., Mackintosh, A., Melbourne-Thomas, J., Muelbert, M.M.C. and Ottersen, G., 2019. Polar Regions. Chapter 3, IPCC Special Report on the Ocean and Cryosphere in a Changing Climate.

Natali, S.M., Schuur, E.A., Trucco, C., Hicks Pries, C.E., Crummer, K.G. and Baron Lopez, A.F., 2011. Effects of experimental warming of air, soil and permafrost on carbon balance in Alaskan tundra. *Global Change Biology*, *17*(3), pp.1394-1407.

Neff, J.C., Finlay, J.C., Zimov, S.A., Davydov, S.P., Carrasco, J.J., Schuur, E.A.G. and Davydova, A.I., 2006. Seasonal changes in the age and structure of dissolved organic carbon in Siberian rivers and streams. *Geophysical Research Letters*, *33*(23).

Neubauer, E., Schenkeveld, W.D., Plathe, K.L., Rentenberger, C., Von Der Kammer, F., Kraemer, S.M. and Hofmann, T., 2013. The influence of pH on iron speciation in podzol extracts: Iron complexes with natural organic matter, and iron mineral nanoparticles. *Science of the total environment*, *461*, pp.108-116.

This article is protected by copyright. All rights reserved.

Neubauer, E., Köhler, S.J., von der Kammer, F., Laudon, H. and Hofmann, T., 2013. Effect of pH and stream order on iron and arsenic speciation in boreal catchments. *Environmental science & technology*, *47*(13), pp.7120-7128

Newman, B.D., Throckmorton, H.M., Graham, D.E., Gu, B., Hubbard, S.S., Liang, L., Wu, Y., Heikoop, J.M., Herndon, E.M., Phelps, T.J. and Wilson, C.J., 2015. Microtopographic and depth controls on active layer chemistry in Arctic polygonal ground. *Geophysical Research Letters*, *42*(6), pp.1808-1817.

Nierop, K.G., Jansen, B. and Verstraten, J.M., 2002. Dissolved organic matter, aluminium and iron interactions: precipitation induced by metal/carbon ratio, pH and competition. *Science of the Total Environment*, *300*(1-3), pp.201-211.

O'Donnell, J.A., Aiken, G.R., Walvoord, M.A. and Butler, K.D., 2012. Dissolved organic matter composition of winter flow in the Yukon River basin: Implications of permafrost thaw and increased groundwater discharge. *Global Biogeochemical Cycles*, *26*(4).

Oelke, C., Zhang, T. and Serreze, M.C., 2004. Modeling evidence for recent warming of the Arctic soil thermal regime. *Geophysical Research Letters*, *31*(7).

Olefeldt, D. and Roulet, N.T., 2012. Effects of permafrost and hydrology on the composition and transport of dissolved organic carbon in a subarctic peatland complex. *Journal of Geophysical Research: Biogeosciences*, *117*(G1).

Oleinikova, O.V., Drozdova, O.Y., Lapitskiy, S.A., Demin, V.V., Bychkov, A.Y. and Pokrovsky, O.S., 2017. Dissolved organic matter degradation by sunlight coagulates organo-mineral colloids and produces low-molecular weight fraction of metals in boreal humic waters. *Geochimica et Cosmochimica Acta*, *211*, pp.97-114.

Oleinikova, O.V., Shirokova, L.S., Gérard, E., Drozdova, O.Y., Lapitskiy, S.A., Bychkov, A.Y. and Pokrovsky, O.S., 2017. Transformation of organo-ferric peat colloids by a heterotrophic bacterium. *Geochimica et cosmochimica acta*, *205*, pp.313-330.

Olsson, P.Q., Sturm, M., Racine, C.H., Romanovsky, V. and Liston, G.E., 2003. Five stages of the Alaskan Arctic cold season with ecosystem implications. *Arctic, Antarctic, and Alpine Research*, *35*(1), pp.74-81.

Opfergelt, S., Williams, H.M., Cornelis, J.T., Guicharnaud, R.A., Georg, R.B., Siebert, C., Gislason, S.R., Halliday, A.N. and Burton, K.W., 2017. Iron and silicon isotope behaviour accompanying weathering in Icelandic soils, and the implications for iron export from peatlands. *Geochimica et Cosmochimica Acta*, *217*, pp.273-291.

Opfergelt, S., 2020. The next generation of climate model should account for the evolution of mineral-organic interactions with permafrost thaw. *Environmental Research Letters*, *15*(9), p.091003.

This article is protected by copyright. All rights reserved.

Opfergelt, S., C. Hirst, E.A. Schuur, E. Mauclet, A. Monhonval, J. Ledman, and Bonanza Creek LTER. 2021. Eight Mile Lake Research Watershed, Thaw Gradient: Geochemical data collected daily in Panguingue Creek during spring thaw and summer rain events, 2018-2019 ver 2. Environmental Data Initiative.

Opfergelt, S., C. Hirst, E.A. Schuur, E. Mauclet, A. Monhonval, J. Ledman, and Bonanza Creek LTER. 2021. Eight Mile Lake Research Watershed, Thaw Gradient: Geochemistry of soil pore waters sampled in May 2018 (0 - 20 cm depth) and August 2019 (0-120 cm depth) at Gradient site, 2018-2019 ver 2. Environmental Data Initiative.

Opfergelt, S., C. Hirst, E.A. Schuur, E. Mauclet, A. Monhonval, J. Ledman, and Bonanza Creek LTER. 2021. Eight Mile Lake Research Watershed, Thaw Gradient: Geochemical data from perched waters collected from boreholes on Gradient site during August-September 2019 ver 2. Environmental Data Initiative.

Osterkamp, T.E., Jorgenson, M.T., Schuur, E.A.G., Shur, Y.L., Kanevskiy, M.Z. and Vogel, J.G., 2007. Physical and Ecological Changes Associated with Warming Permafrost. *Climatic change*.

Osterkamp, T.E., Jorgenson, M.T., Schuur, E.A.G., Shur, Y.L., Kanevskiy, M.Z., Vogel, J.G. and Tumskoy, V.E., 2009. Physical and ecological changes associated with warming permafrost and thermokarst in interior Alaska. *Permafrost and Periglacial Processes*, *20*(3), pp.235-256.

Overduin, P.P., Kane, D.L. and van Loon, W.K., 2006. Measuring thermal conductivity in freezing and thawing soil using the soil temperature response to heating. *Cold Regions Science and Technology*, *45*(1), pp.8-22.

Page, S.E., Kling, G.W., Sander, M., Harrold, K.H., Logan, J.R., McNeill, K. and Cory, R.M., 2013. Dark formation of hydroxyl radical in arctic soil and surface waters. *Environmental science & technology*, *47*(22), pp.12860-12867.

Page, S.E., Logan, J.R., Cory, R.M. and McNeill, K., 2014. Evidence for dissolved organic matter as the primary source and sink of photochemically produced hydroxyl radical in arctic surface waters. *Environmental Science: Processes & Impacts*, *16*(4), pp.807-822.

Patzner, M.S., Mueller, C.W., Malusova, M., Baur, M., Nikeleit, V., Scholten, T., Hoeschen, C., Byrne, J., Borch, T. and Kappler, A., 2020. Iron mineral dissolution releases iron and associated organic carbon during permafrost thaw.

Pegoraro, E.F., Mauritz, M.E., Ogle, K., Ebert, C.H. and Schuur, E.A., 2020. Lower soil moisture and deep soil temperatures in thermokarst features increase old soil carbon loss after 10 years of experimental permafrost warming. *Global Change Biology*.

Peng, X., Frauenfeld, O.W., Cao, B., Wang, K., Wang, H., Su, H., Huang, Z., Yue, D. and Zhang, T., 2016. Response of changes in seasonal soil freeze/thaw state to climate change from

This article is protected by copyright. All rights reserved.

Accepted Article

1950 to 2010 across china. *Journal of Geophysical Research: Earth Surface*, *121*(11), pp.1984-2000.

Peng, X., Zhang, T., Frauenfeld, O.W., Wang, K., Luo, D., Cao, B., Su, H., Jin, H. and Wu, Q., 2018. Spatiotemporal changes in active layer thickness under contemporary and projected climate in the Northern Hemisphere. *Journal of Climate*, *31*(1), pp.251-266.

Petrone, K.C., Jones, J.B., Hinzman, L.D. and Boone, R.D., 2006. Seasonal export of carbon, nitrogen, and major solutes from Alaskan catchments with discontinuous permafrost. *Journal of Geophysical Research: Biogeosciences*, *111*(G2).

Plaza, C., Pegoraro, E., Bracho, R., Celis, G., Crummer, K.G., Hutchings, J.A., Pries, C.E.H., Mauritz, M., Natali, S.M., Salmon, V.G. and Schädel, C., 2019. Direct observation of permafrost degradation and rapid soil carbon loss in tundra. *Nature Geoscience*, *12*(8), pp.627-631.

Pokrovsky, O.S. and Schott, J., 2002. Iron colloids/organic matter associated transport of major and trace elements in small boreal rivers and their estuaries (NW Russia). *Chemical Geology*, *190*(1-4), pp.141-179.

Pokrovsky, O.S., Schott, J. and Dupré, B., 2006. Trace element fractionation and transport in boreal rivers and soil porewaters of permafrost-dominated basaltic terrain in Central Siberia. *Geochimica et Cosmochimica Acta*, *70*(13), pp.3239-3260.

Pokrovsky, O.S., Viers, J., Shirokova, L.S., Shevchenko, V.P., Filipov, A.S. and Dupré, B., 2010. Dissolved, suspended, and colloidal fluxes of organic carbon, major and trace elements in the Severnaya Dvina River and its tributary. *Chemical Geology*, *273*(1-2), pp.136-149.

Pokrovsky, O.S., Reynolds, B.C., Prokushkin, A.S., Schott, J. and Viers, J., 2013. Silicon isotope variations in Central Siberian rivers during basalt weathering in permafrost-dominated larch forests. *Chemical Geology*, *355*, pp.103-116.

Pokrovsky, O.S., Loiko, S.V., Shirokova, L.S., Kritskov, I.V., Kolesnichenko, L.G., Kopysov, S.G., Zemtsov, V.A., Kulizhsky, S.P., Vorobyev, S.N., Manasypov, R.M. and Pokrovsky, B.G., 2015. Permafrost coverage, watershed area and season control of dissolved carbon and major elements in western Siberian rivers.

Pokrovsky, O.S., Manasypov, R.M., Loiko, S.V. and Shirokova, L.S., 2016. Organic and organo-mineral colloids in discontinuous permafrost zone. *Geochimica et Cosmochimica Acta*, *188*, pp.1-20.

Pokrovsky, O.S., Manasypov, R.M., Loiko, S.V., Krickov, I.A., Kopysov, S.G., Kolesnichenko, L.G., Vorobyev, S.N. and Kirpotin, S.N., 2016. Trace element transport in western Siberian rivers across a permafrost gradient. *Biogeosciences*, *13*(6), pp.1877-1900.

Pokrovsky, O.S., Manasypov, R.M., Loiko, S.V. and Shirokova, L.S., 2016. Organic and organo-mineral colloids in discontinuous permafrost zone. *Geochimica et Cosmochimica Acta*, *188*, pp.1-20.

This article is protected by copyright. All rights reserved.

Accepted Article

Pokrovsky, O.S., 2016. Measuring and estimating fluxes of carbon, major and trace elements to the Arctic Ocean. In *Novel Methods for Monitoring and Managing Land and Water Resources in Siberia* (pp. 185-212). Springer, Cham.

Porcal, P., Amirbahman, A., Kopáček, J., Novák, F. and Norton, S.A., 2009. Photochemical release of humic and fulvic acid-bound metals from simulated soil and streamwater. *Journal of Environmental Monitoring*, *11*(5), pp.1064-1071

Porcelli, D., Andersson, P.S., Wasserburg, G.J., Ingri, J. and Baskaran, M., 1997. The importance of colloids and mires for the transport of uranium isotopes through the Kalix River watershed and Baltic Sea. *Geochimica et Cosmochimica Acta*, *61*(19), pp.4095-4113.

Pries, C.E.H., Schuur, E.A. and Crummer, K.G., 2012. Holocene carbon stocks and carbon accumulation rates altered in soils undergoing permafrost thaw. *Ecosystems*, *15*(1), pp.162-173.

Prokushkin, A.S., Kajimoto, T., Prokushkin, S.G., McDowell, W.H., Abaimov, A.P. and Matsuura, Y., 2005. Climatic factors influencing fluxes of dissolved organic carbon from the forest floor in a continuous-permafrost Siberian watershed. *Canadian Journal of Forest Research*, *35*(9), pp.2130-2140.

Prokushkin, A.S., Kawahigashi, M. and Tokareva, I.V., 2009. Global warming and dissolved organic carbon release from permafrost soils. In *Permafrost soils* (pp. 237-250). Springer, Berlin, Heidelberg.

Quinton, W.L. and Marsh, P., 1998. The influence of mineral earth hummocks on subsurface drainage in the continuous permafrost zone. *Permafrost and Periglacial Processes*, *9*(3), pp.213-228.

Raudina, T.V., Loiko, S.V., Lim, A.G., Krickov, I.V., Shirokova, L.S., Istigechev, G.I., Kuzmina, D.M., Kulizhsky, S.P., Vorobyev, S.N. and Pokrovsky, O.S., 2017. Dissolved organic carbon and major and trace elements in peat porewater of sporadic, discontinuous, and continuous permafrost zones of western Siberia. *Biogeosciences*, *14*(14), pp.3561-3584.

Raudina, T.V., Loiko, S.V., Kuzmina, D.M., Shirokova, L.S., Kulizhskiy, S.P., Golovatskaya, E.A. and Pokrovsky, O.S., 2021. Colloidal organic carbon and trace elements in peat porewaters across a permafrost gradient in Western Siberia. *Geoderma*, *390*, p.114971.

Raymond, P.A., McClelland, J.W., Holmes, R.M., Zhulidov, A.V., Mull, K., Peterson, B.J., Striegl, R.G., Aiken, G.R. and Gurtovaya, T.Y., 2007. Flux and age of dissolved organic carbon exported to the Arctic Ocean: A carbon isotopic study of the five largest arctic rivers. *Global Biogeochemical Cycles*, *21*(4).

Raymond, P.A., Saiers, J.E. and Sobczak, W.V., 2016. Hydrological and biogeochemical controls on watershed dissolved organic matter transport: Pulse- shunt concept. *Ecology*, *97*(1), pp.5-16.

This article is protected by copyright. All rights reserved.

Rember, R.D. and Trefry, J.H., 2004. Increased concentrations of dissolved trace metals and organic carbon during snowmelt in rivers of the Alaskan Arctic. *Geochimica et Cosmochimica Acta*, *68*(3), pp.477-489.

Riedel, T., Zak, D., Biester, H. and Dittmar, T., 2013. Iron traps terrestrially derived dissolved organic matter at redox interfaces. *Proceedings of the National Academy of Sciences*, *110*(25), pp.10101-10105.

Rowland, J.C., Jones, C.E., Altmann, G., Bryan, R., Crosby, B.T., Hinzman, L.D., Kane, D.L., Lawrence, D.M., Mancino, A., Marsh, P. and McNamara, J.P., 2010. Arctic landscapes in transition: responses to thawing permafrost. *Eos, Transactions American Geophysical Union*, *91*(26), pp.229-230.

Rowley, M.C., Grand, S. and Verrecchia, É.P., 2018. Calcium-mediated stabilisation of soil organic carbon. *Biogeochemistry*, *137*(1-2), pp.27-49.

Schmitt-Kopplin, P., Hertkorn, N., Schulten, H.R. and Kettrup, A., 1998. Structural changes in a dissolved soil humic acid during photochemical degradation processes under O2 and N2 atmosphere. *Environmental science & technology*, *32*(17), pp.2531-2541.

Schuur, E.A., Crummer, K.G., Vogel, J.G. and Mack, M.C., 2007. Plant species composition and productivity following permafrost thaw and thermokarst in Alaskan tundra. *Ecosystems*, *10*(2), pp.280-292.

Schuur, E.A., Vogel, J.G., Crummer, K.G., Lee, H., Sickman, J.O. and Osterkamp, T.E., 2009. The effect of permafrost thaw on old carbon release and net carbon exchange from tundra. *Nature*, *459*(7246), pp.556-559.

Schuur, E.A., McGuire, A.D., Schädel, C., Grosse, G., Harden, J.W., Hayes, D.J., Hugelius, G., Koven, C.D., Kuhry, P., Lawrence, D.M. and Natali, S.M., 2015. Climate change and the permafrost carbon feedback. *Nature*, *520*(7546), pp.171-179.

Schwab, M.S., Hilton, R.G., Raymond, P.A., Haghipour, N., Amos, E., Tank, S.E., Holmes, R.M., Tipper, E.T. and Eglinton, T.I., 2020. An abrupt aging of dissolved organic carbon in large Arctic rivers. *Geophysical research letters*, *47*(23), p.e2020GL088823.

Serikova, S., Pokrovsky, O.S., Ala-Aho, P., Kazantsev, V., Kirpotin, S.N., Kopysov, S.G., Krickov, I.V., Laudon, H., Manasypov, R.M., Shirokova, L.S. and Soulsby, C., 2018. High riverine CO 2 emissions at the permafrost boundary of Western Siberia. *Nature Geoscience*, *11*(11), pp.825-829.

Shakil, S., Tank, S.E., Kokelj, S.V., Vonk, J.E. and Zolkos, S., 2020. Particulate dominance of organic carbon mobilization from thaw slumps on the Peel Plateau, NT: Quantification and implications for stream systems and permafrost carbon release. *Environmental Research Letters*, *15*(11), p.114019.

This article is protected by copyright. All rights reserved.

Accepted Article

Shirokova, L.S., Pokrovsky, O.S., Kirpotin, S.N., Desmukh, C., Pokrovsky, B.G., Audry, S. and Viers, J., 2013. Biogeochemistry of organic carbon, CO 2, CH 4, and trace elements in thermokarst water bodies in discontinuous permafrost zones of Western Siberia. *Biogeochemistry*, *113*(1-3), pp.573-593.

Shiller, A.M., Duan, S., van Erp, P. and Bianchi, T.S., 2006. Photo- oxidation of dissolved organic matter in river water and its effect on trace element speciation. *Limnology and Oceanography*, *51*(4), pp.1716-1728.

Shogren, A.J., Zarnetske, J.P., Abbott, B.W., Iannucci, F. and Bowden, W.B., 2020. We cannot shrug off the shoulder seasons: Addressing knowledge and data gaps in an Arctic Headwater. *Environmental Research Letters*, *15*(10), p.104027.

Shur, Y., Hinkel, K.M. and Nelson, F.E., 2005. The transient layer: implications for geocryology and climate- change science. *Permafrost and Periglacial Processes*, *16*(1), pp.5-17.

Sjöstedt, C.S., Gustafsson, J.P. and Köhler, S.J., 2010. Chemical equilibrium modeling of organic acids, pH, aluminum, and iron in Swedish surface waters. *Environmental science & technology*, *44*(22), pp.8587-8593.

Soil Survey Staff (1999), Soil Taxonomy: A Basic System of Soil Classification for Making and Interpreting Soil Surveys. Agricultural Handbook, vol. 436, Natl. Res. Conserv. Serv., USDA, Washington, D. C.

Spencer, R.G., Aiken, G.R., Wickland, K.P., Striegl, R.G. and Hernes, P.J., 2008. Seasonal and spatial variability in dissolved organic matter quantity and composition from the Yukon River basin, Alaska. *Global Biogeochemical Cycles*, *22*(4).

Spencer, R.G., Aiken, G.R., Butler, K.D., Dornblaser, M.M., Striegl, R.G. and Hernes, P.J., 2009. Utilizing chromophoric dissolved organic matter measurements to derive export and reactivity of dissolved organic carbon exported to the Arctic Ocean: A case study of the Yukon River, Alaska. *Geophysical Research Letters*, *36*(6).

Stepanova, V.A., Pokrovsky, O.S., Viers, J., Mironycheva-Tokareva, N.P., Kosykh, N.P. and Vishnyakova, E.K., 2015. Elemental composition of peat profiles in western Siberia: Effect of the micro-landscape, latitude position and permafrost coverage. *Applied Geochemistry*, *53*, pp.53-70.

Stone, R.S., Dutton, E.G., Harris, J.M. and Longenecker, D., 2002. Earlier spring snowmelt in northern Alaska as an indicator of climate change. *Journal of Geophysical Research: Atmospheres*, *107*(D10), pp.ACL-10.

Streletskiy, D.A., Tananaev, N.I., Opel, T., Shiklomanov, N.I., Nyland, K.E., Streletskaya, I.D. and Shiklomanov, A.I., 2015. Permafrost hydrology in changing climatic conditions: seasonal variability of stable isotope composition in rivers in discontinuous permafrost. *Environmental Research Letters*, *10*(9), p.095003.

This article is protected by copyright. All rights reserved.

Accepted Article

Stendel, M. and Christensen, J.H., 2002. Impact of global warming on permafrost conditions in a coupled GCM. *Geophysical Research Letters*, *29*(13), pp.10-1.

Stocker, T.F., Qin, D., Plattner, G.K., Tignor, M.M., Allen, S.K., Boschung, J., Nauels, A., Xia, Y., Bex, V. and Midgley, P.M., 2014. Climate Change 2013: The physical science basis. contribution of working group I to the fifth assessment report of IPCC the intergovernmental panel on climate change.

Stocker, T.F., Qin, D., Plattner, G.K., Tignor, M.M., Allen, S.K., Boschung, J., Nauels, A., Xia, Y., Bex, V. and Midgley, P.M., 2014. Climate Change 2013: The physical science basis. contribution of working group I to the fifth assessment report of IPCC the intergovernmental panel on climate change.

Stolpe, B., Guo, L., Shiller, A.M. and Aiken, G.R., 2013. Abundance, size distributions and trace-element binding of organic and iron-rich nanocolloids in Alaskan rivers, as revealed by field-flow fractionation and ICP-MS. *Geochimica et Cosmochimica Acta*, *105*, pp.221-239.

Stolpe, B. and Hassellöv, M., 2007. Changes in size distribution of fresh water nanoscale colloidal matter and associated elements on mixing with seawater. *Geochimica et Cosmochimica Acta*, *71*(13), pp.3292-3301.

Striegl, R.G., Aiken, G.R., Dornblaser, M.M., Raymond, P.A. and Wickland, K.P., 2005. A decrease in discharge- normalized DOC export by the Yukon River during summer through autumn. *Geophysical Research Letters*, *32*(21).

Striegl, R.G., Dornblaser, M.M., Aiken, G.R., Wickland, K.P. and Raymond, P.A., 2007. Carbon export and cycling by the Yukon, Tanana, and Porcupine rivers, Alaska, 2001–2005. *Water Resources Research*, *43*(2).

Stumm, W. and Morgan, J.J., 2012. *Aquatic chemistry: chemical equilibria and rates in natural waters* (Vol. 126). John Wiley & Sons.

Sundman, A., Karlsson, T., Laudon, H. and Persson, P., 2014. XAS study of iron speciation in soils and waters from a boreal catchment. *Chemical Geology*, *364*, pp.93-102.

Tipping, E., Rey-Castro, C., Bryan, S.E. and Hamilton-Taylor, J., 2002. Al (III) and Fe (III) binding by humic substances in freshwaters, and implications for trace metal speciation. *Geochimica et Cosmochimica Acta*, *66*(18), pp.3211-3224.

Townsend-Small, A., McClelland, J.W., Holmes, R.M. and Peterson, B.J., 2011. Seasonal and hydrologic drivers of dissolved organic matter and nutrients in the upper Kuparuk River, Alaskan Arctic. *Biogeochemistry*, *103*(1-3), pp.109-124.

Tranvik, L.J., 1988. Availability of dissolved organic carbon for planktonic bacteria in oligotrophic lakes of differing humic content. *Microbial Ecology*, *16*(3), pp.311-322.

This article is protected by copyright. All rights reserved.

Accepted Article

Tranvik, L., 1994. Effects of colloidal organic matter on the growth of bacteria and protists in lake water. *Limnology and oceanography*, *39*(6), pp.1276-1285.

Vasyukova, E.V., Pokrovsky, O.S., Viers, J., Oliva, P., Dupré, B., Martin, F. and Candaudap, F., 2010. Trace elements in organic-and iron-rich surficial fluids of the boreal zone: Assessing colloidal forms via dialysis and ultrafiltration. *Geochimica et Cosmochimica Acta*, *74*(2), pp.449-468.

Vasyukova, E., Pokrovsky, O.S., Viers, J. and Dupré, B., 2012. New operational method of testing colloid complexation with metals in natural waters. *Applied geochemistry*, *27*(6), pp.1226-1237.

Vogel, J., Schuur, E.A., Trucco, C. and Lee, H., 2009. Response of CO2 exchange in a tussock tundra ecosystem to permafrost thaw and thermokarst development. *Journal of Geophysical Research: Biogeosciences*, *114*(G4).

Vonk, J.E., Mann, P.J., Davydov, S., Davydova, A., Spencer, R.G., Schade, J., Sobczak, W.V., Zimov, N., Zimov, S., Bulygina, E. and Eglinton, T.I., 2013. High biolability of ancient permafrost carbon upon thaw. *Geophysical Research Letters*, *40*(11), pp.2689-2693.

Vonk, J.E., Tank, S.E. and Walvoord, M.A., 2019. Integrating hydrology and biogeochemistry across frozen landscapes. *Nature communications*, *10*(1), pp.1-4.

Ward, C.P. and Cory, R.M., 2020. Assessing the prevalence, products, and pathways of dissolved organic matter partial photo-oxidation in arctic surface waters. *Environmental Science: Processes & Impacts*, *22*(5), pp.1214-1223.

Ward, C.P. and Cory, R.M., 2016. Complete and partial photo-oxidation of dissolved organic matter draining permafrost soils. *Environmental science & technology*, *50*(7), pp.3545-3553.

Wickland, K.P., Waldrop, M.P., Aiken, G.R., Koch, J.C., Jorgenson, M.T. and Striegl, R.G., 2018. Dissolved organic carbon and nitrogen release from boreal Holocene permafrost and seasonally frozen soils of Alaska. *Environmental Research Letters*, *13*(6), p.065011.

Wickland, K.P., Aiken, G.R., Butler, K., Dornblaser, M.M., Spencer, R.G.M. and Striegl, R.G., 2012. Biodegradability of dissolved organic carbon in the Yukon River and its tributaries: Seasonality and importance of inorganic nitrogen. *Global Biogeochemical Cycles*, *26*(4).

Wu, Q. and Zhang, T., 2010. Changes in active layer thickness over the Qinghai- Tibetan Plateau from 1995 to 2007. *Journal of Geophysical Research: Atmospheres*, *115*(D9).

Yeghicheyan, D., Carignan, J., Valladon, M., Le Coz, M.B., Cornec, F.L., Castrec- Rouelle, M., Robert, M., Aquilina, L., Aubry, E., Churlaud, C. and Dia, A., 2001. A compilation of silicon and thirty one trace elements measured in the natural river water reference material SLRS- 4 (NRC- CNRC). *Geostandards newsletter*, *25*(2- 3), pp.465-474.

This article is protected by copyright. All rights reserved.

Zhang, T., Frauenfeld, O.W., Serreze, M.C., Etringer, A., Oelke, C., McCreight, J., Barry, R.G., Gilichinsky, D., Yang, D., Ye, H. and Ling, F., 2005. Spatial and temporal variability in active layer thickness over the Russian Arctic drainage basin. *Journal of Geophysical Research: Atmospheres*, *110*(D16).

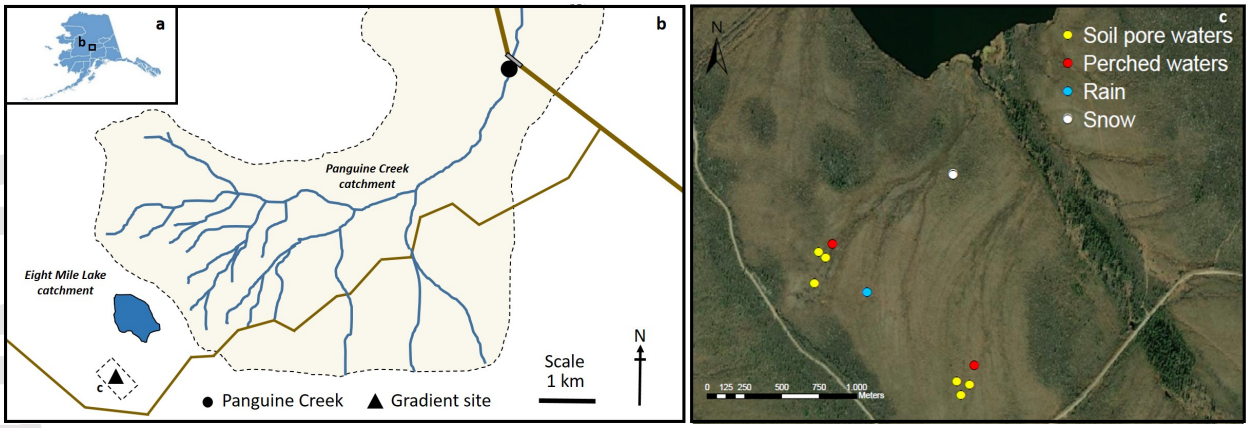
Zhang, T., Barry, R.G., Knowles, K., Heginbottom, J.A. and Brown, J., 1999. Statistics and characteristics of permafrost and ground- ice distribution in the Northern Hemisphere. *Polar Geography*, *23*(2), pp.132-154.

Zhang, X., Hutchings, J.A., Bianchi, T.S., Liu, Y., Arellano, A.R. and Schuur, E.A., 2017. Importance of lateral flux and its percolation depth on organic carbon export in Arctic tundra soil: Implications from a soil leaching experiment. *Journal of Geophysical Research: Biogeosciences*, *122*(4), pp.796-810.

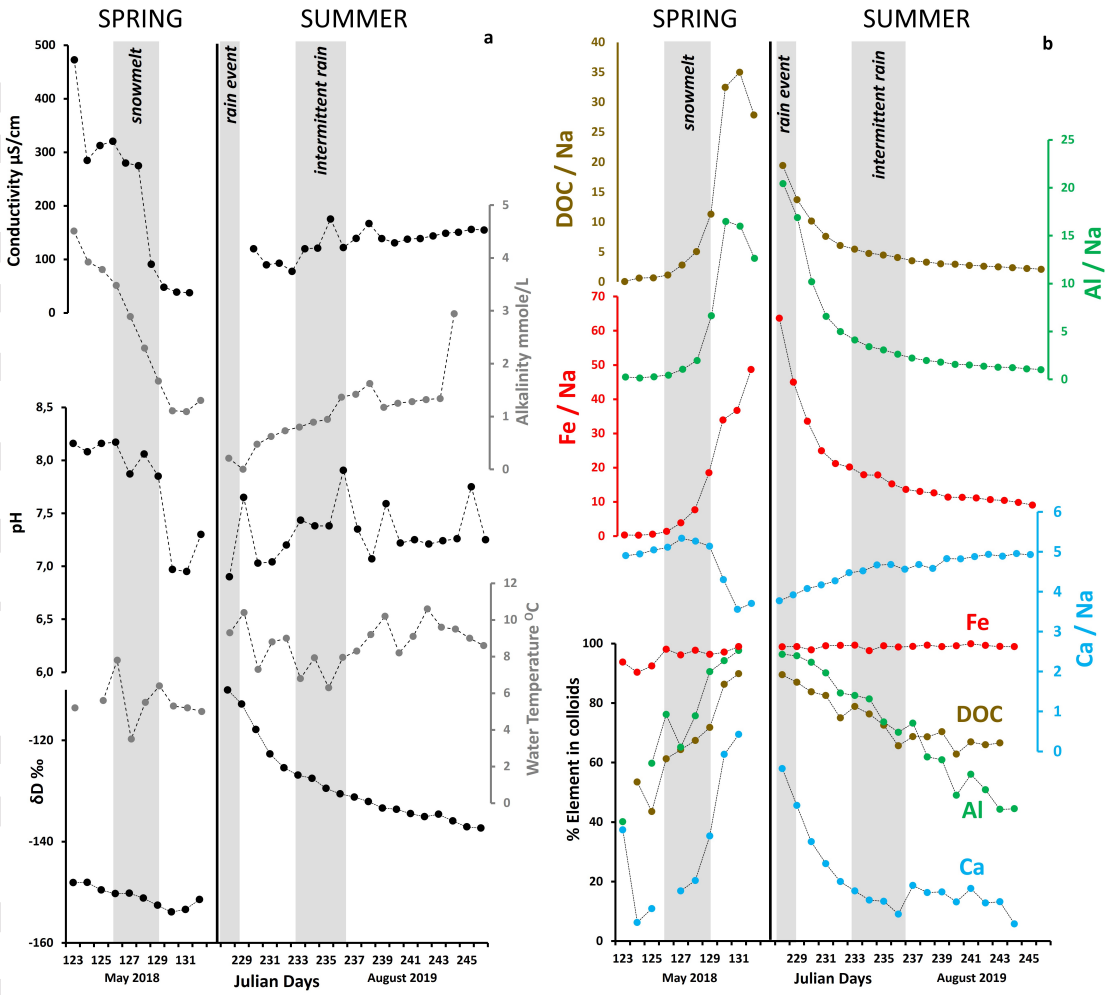
Accepted Article

This article is protected by copyright. All rights reserved.

Accepted Article



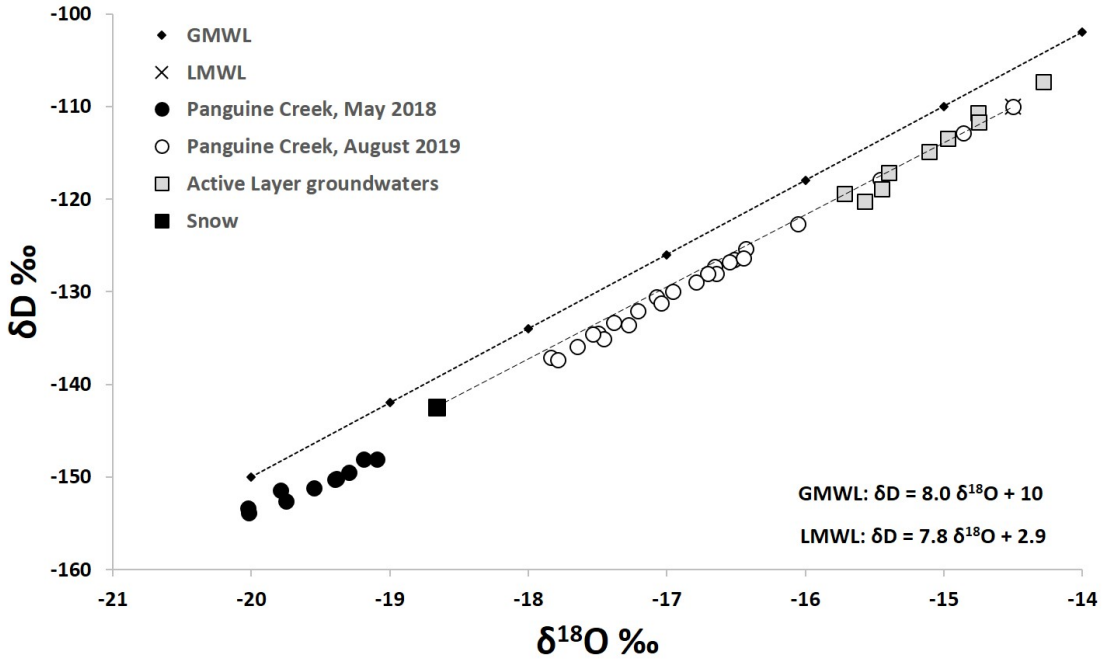
This article is protected by copyright. All rights reserved.



Accepted Article

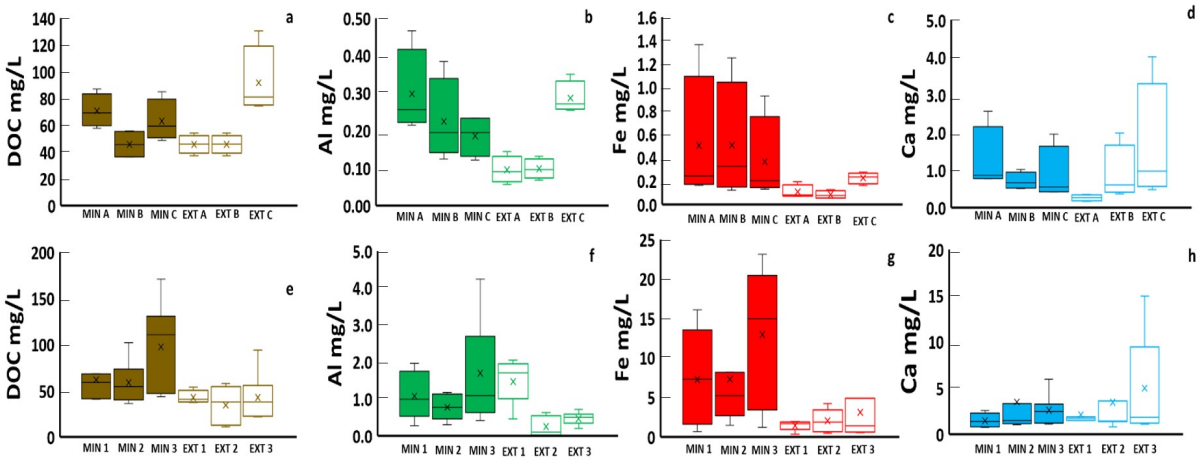
This article is protected by copyright. All rights reserved.

Accepted Article



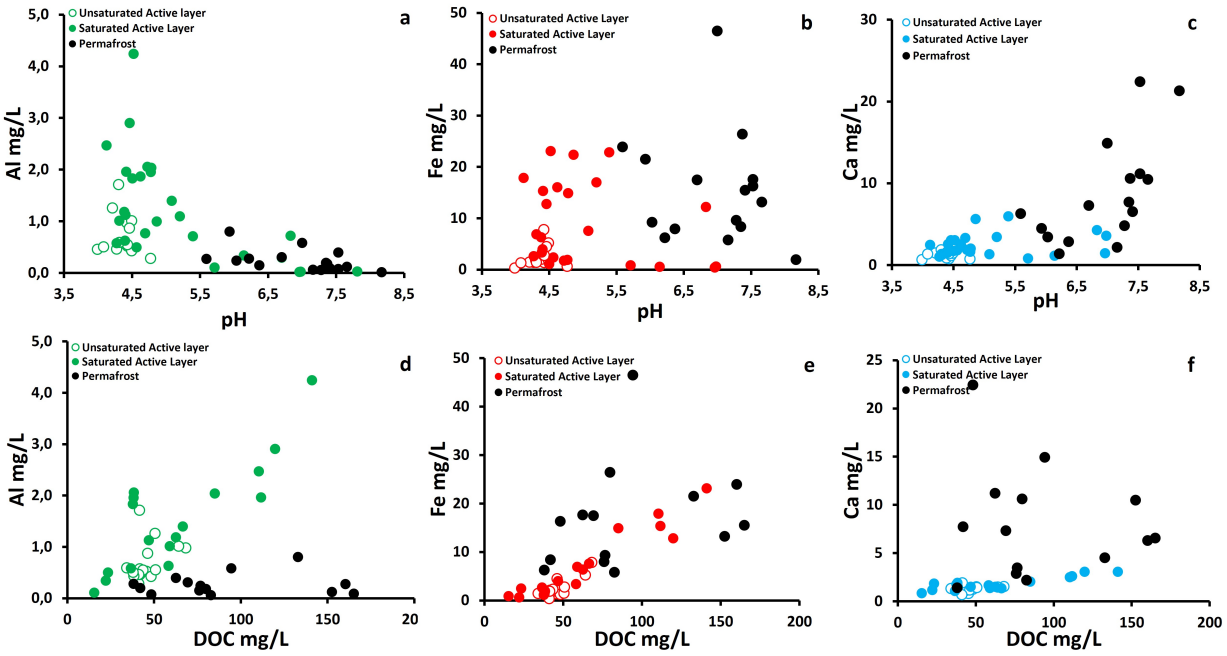
This article is protected by copyright. All rights reserved.

Accepted Article



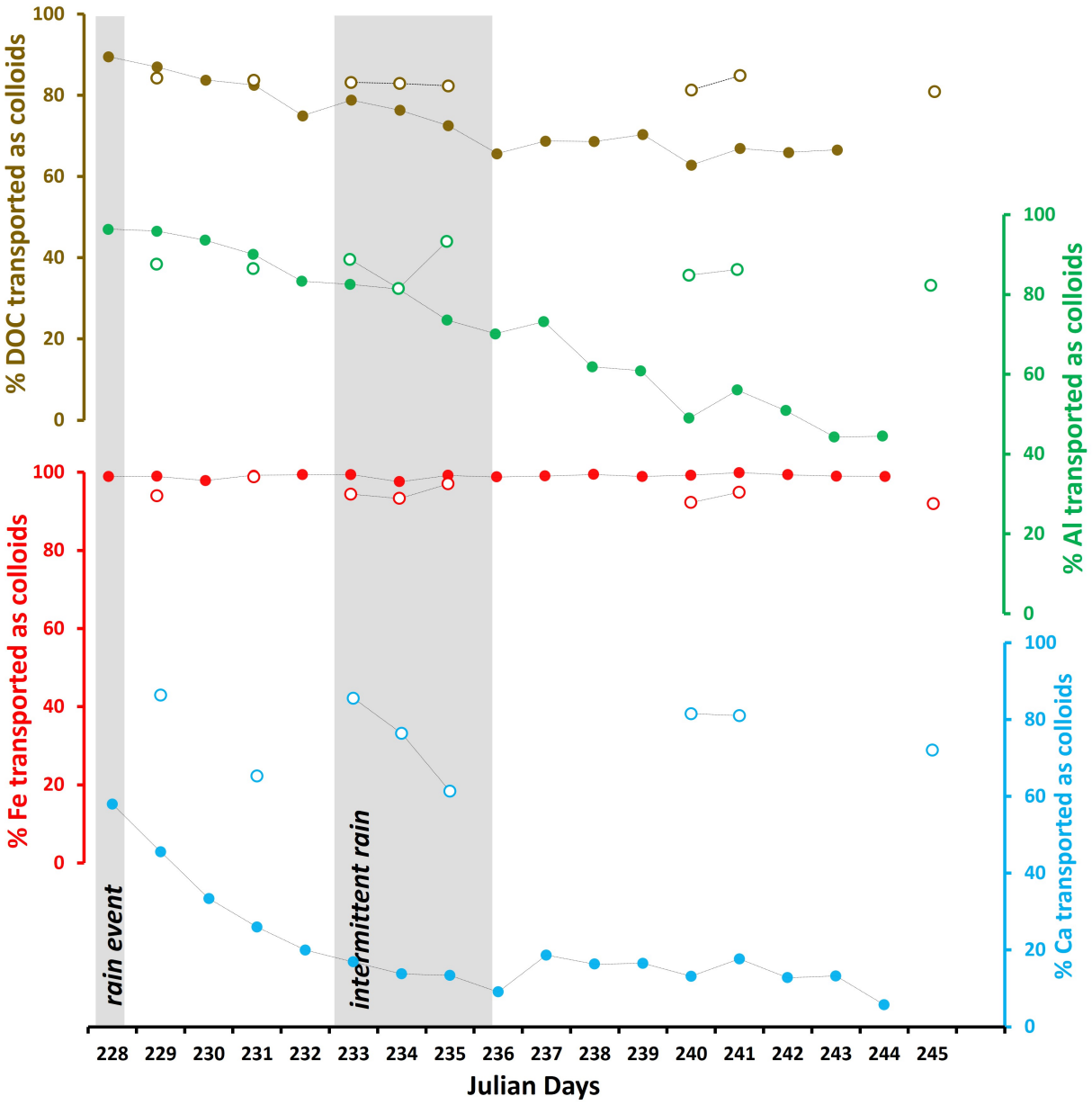
This article is protected by copyright. All rights reserved.

Accepted Article

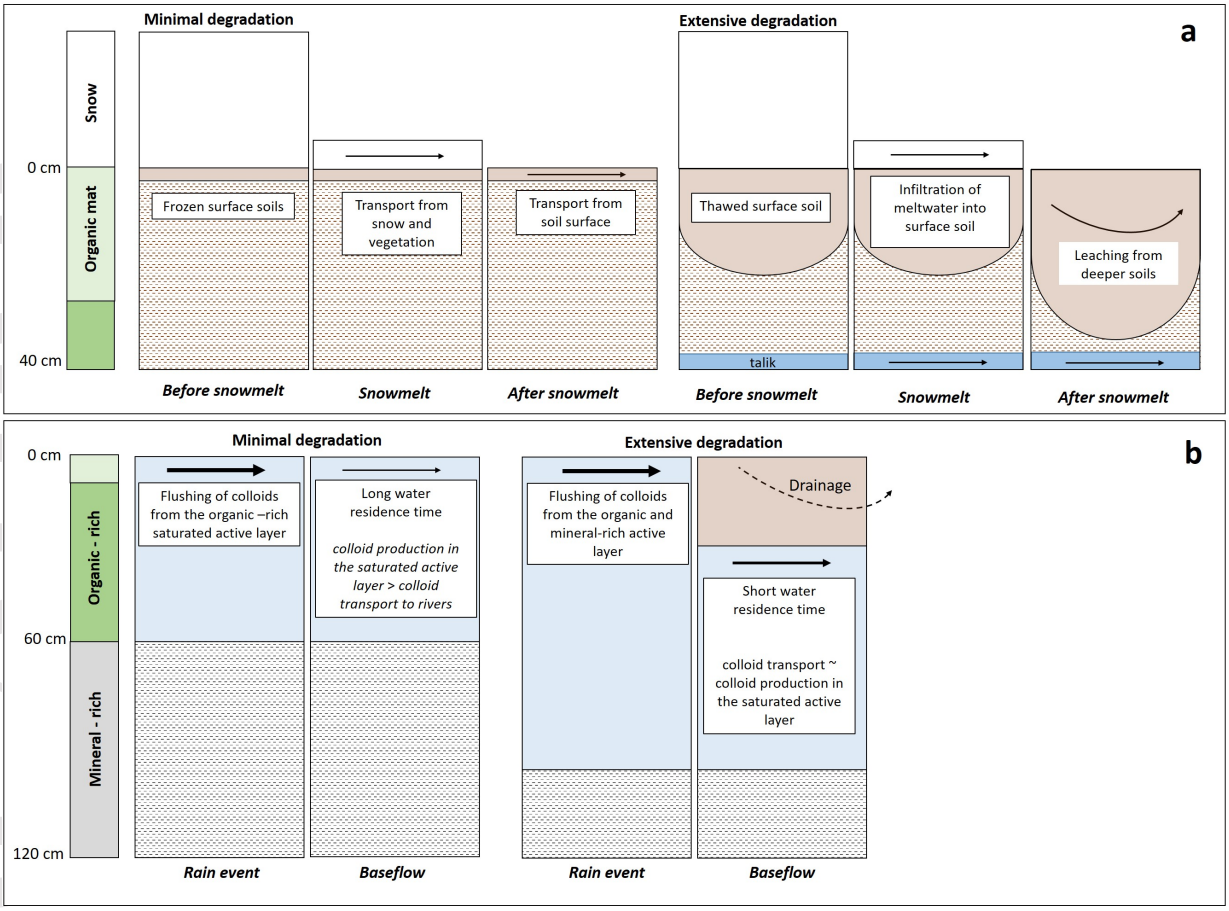


This article is protected by copyright. All rights reserved.

Accepted Article

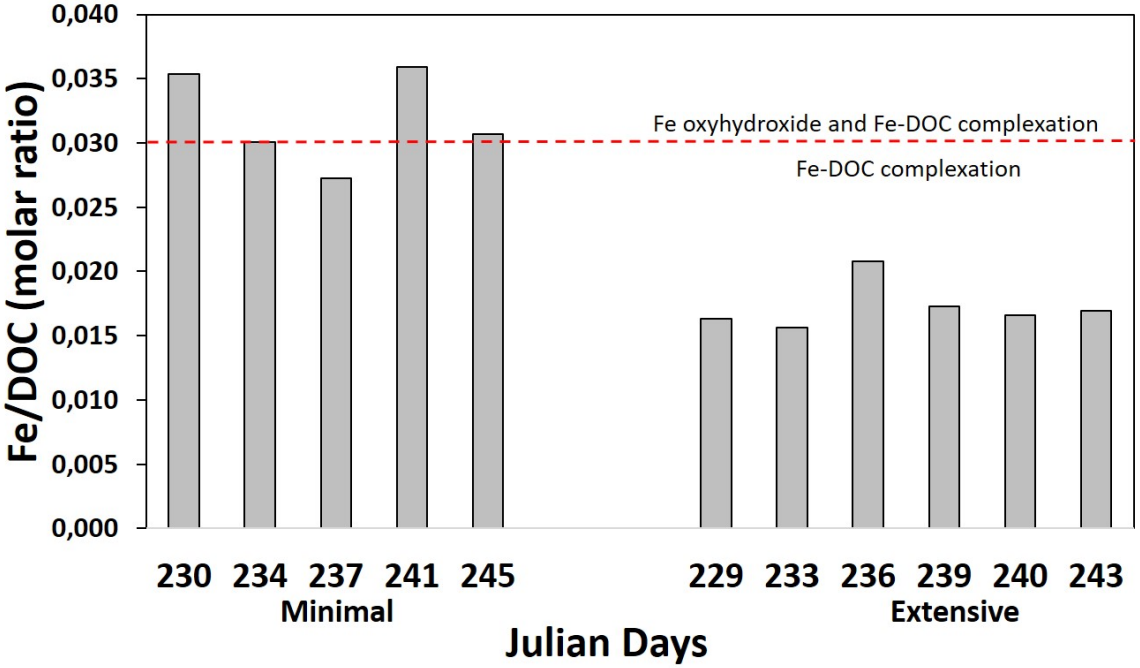


This article is protected by copyright. All rights reserved.



Accepted Article

This article is protected by copyright. All rights reserved.



Accepted Article

This article is protected by copyright. All rights reserved.

Accepted Article

[Global Biogeochemical Cycles]

Supporting Information for

Seasonal changes in hydrology and permafrost degradation control mineral element-bound DOC transport from permafrost soils to streams

Catherine Hirst[1], Elisabeth Mauclet[1], Arthur Monhonval[1], Emeline Tihon[1], Justin Ledman[2], Edward. A.G. Schuur[2], Sophie Opfergelt[1]

[1]Earth and Life Institute, Université catholique de Louvain, Louvain-la-Neuve, Belgium
[2]Center for Ecosystem Science and Society, Northern Arizona University, Flagstaff, AZ, USA

Contents of this file

Text S1
Figures S1 to S4
Tables S1

Introduction

The supporting information includes one section of text, four figures and one table. The text outlines the reasoning for the choice of sampling sites in the study. Data in SI Figure 1 – 3 were obtained from the Bonanza Creek LTER database: https://www.lter.uaf.edu/data. Data in SI Figure 4 were obtained using geochemical modelling program:Visual MINTEQ (Gustafsson et al., 2011). Data in Table 1 show statistical data determined using the Welch T-test in the program Microsoft Excel.

This article is protected by copyright. All rights reserved.

Accepted Article

Text S1.

To set up sites with contrasted conditions of permafrost degradation, we investigated available soil temperature, soil moisture, active layer thickness (ALT), and water table depths (WTD) data from Gradient site, which are reported in the Bonanza Creek LTER database (https://www.lter.uaf.edu/data).

In May 2018, during snowmelt and flooding, there are contrasting soil temperature and soil moisture contents at MIN and EXT sites (S.I. Figure 1). Between May 3-May 12 2018, at MIN sites the mean daily soil temperature at 20 cm depth remained below 0°C throughout baseflow (-0.15 ± 0.02°C on May 3), snowmelt (-0.10 ± 0.01°C on May 6) and flooding conditions (-0.02 ± 0.02°C on May 12). In contrast, at EXT sites the mean daily soil temperature at 20 cm increased from below 0°C to above 0°C at the same time as snowmelt occurred (-0.41 ± 0.09°C during baseflow, 0.21 ± 0.08 °C during snowmelt and 0.18 ± 0.03 °C during flooding conditions). Between May 3-May 12 2018, at MIN sites the mean daily soil moisture content in the 0-15 cm of soil remained relatively constant between baseflow and flooding (0.278 ± 0.005 % on May 3, 0.276 ± 0.001 % on May 6 and 0.278 ± 0.004 % on May 12). In contrast, at EXT sites soil moisture increased during the period of snowmelt and flooding (0.291 ± 0.001 % on May 3, 0.289 ± 0.001 % on May 6 and 0.394 ± 0.179 % on May 12).

In August-September 2019, we performed measurements of ALT and WTD in boreholes and soil profiles at sites of minimal and extensive degradation on Gradient site using the same methodology reported in the Bonanza Creek database (in MIN and in EXT: n = 6 boreholes, n = 3 soil profiles): ALT was determined using a metal probe that was pushed into the soil to the active layer-permafrost boundary, and the WTD was measured relative to the ground surface at boreholes and soil sampling sites using a meter stick. Boreholes are located within 20 m of the soil profile sites, and the data obtained were compared with ALT and WTD data reported in the Bonanza Creek LTER database. The deepest ALT measurements are similar to the deepest reported measurements in 2019 (114 cm, September 14 2019) showing that samples were collected at the point of maximum thaw in 2019. The ALT in soil samples at MIN sites (MIN 1, 2, 3: 55, 68, 60 cm, respectively)

This article is protected by copyright. All rights reserved.

lie within the standard deviation of those measured at monitored sites (67±7 cm) whereas the values at EXT sites (EXT 1, 2, 3 : 48, 96, 65 cm) are lower than the values reported at monitored sites (107±17 cm; S.I. Figure 2a, b). The WTD in soil samples at MIN sites (MIN 1, 2, 3: 25, 23, 14 cm) are lower than the range of values reported at monitored sites (-6 ± 6 cm) whereas the WTD at EXT sites (EXT 1, 2, 3: 22, 8, -29 cm) lie within the range of those reported at monitored sites (-13±9 cm). Water table depth at MIN and EXT sites show contrasting response to the rain event to baseflow transition (S.I. Figure 3). In boreholes at MIN site, there was no overall decrease or increase in WTD between rain event and baseflow conditions for all boreholes. In contrast, boreholes at EXT site show a 52 % decrease in water table (n = 6 plots, S.D. = 22 %) from the rain event to summer baseflow (S.I. Figure. 2c, d).

Accepted Article

This article is protected by copyright. All rights reserved.

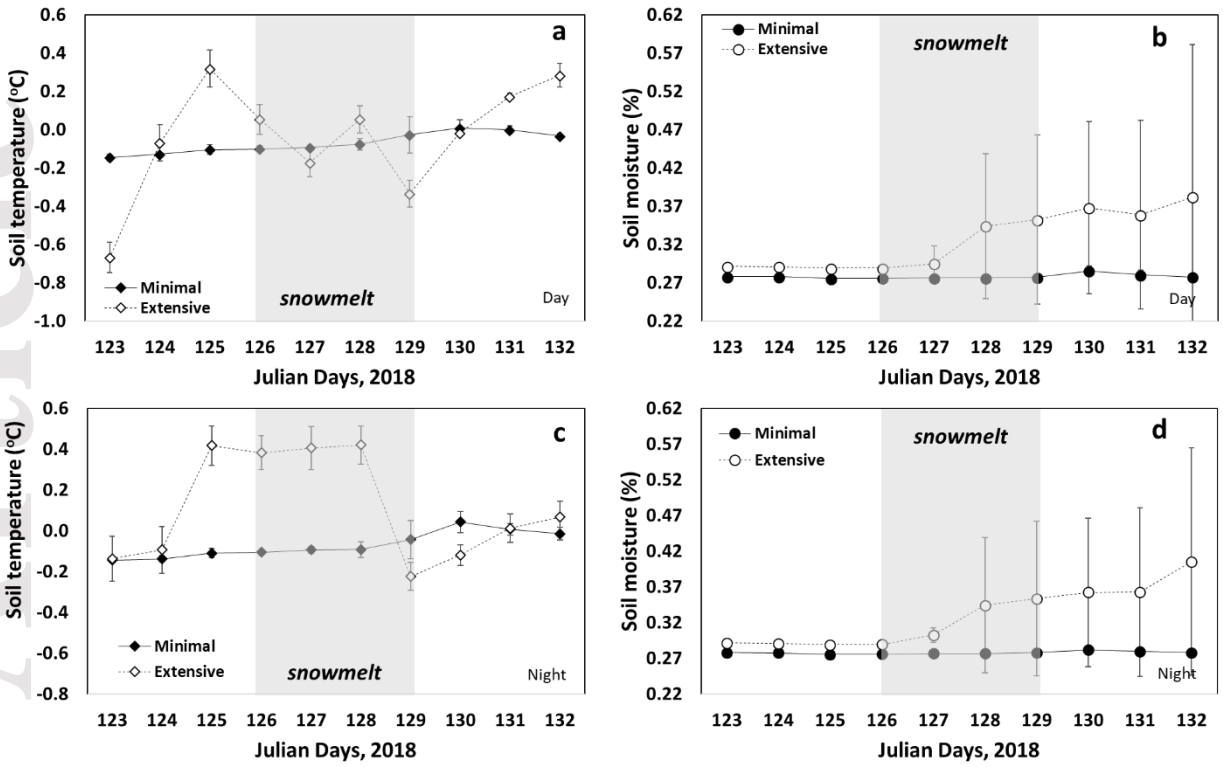


Figure S1. A time series of soil temperature (a and b) and soil moisture (c and d) at sites of minimal (MIN) and extensive (EXT) permafrost degradation, between May 3 2018 and May 12 2018. Soil temperature at 20 cm is shown and is the average of data collected every 30 minutes at 3 plots on Gradient site. The soil moisture measured between 0-20 cm is shown and is the average of data collected every 30 minutes at 3 plots on Gradient site. The standard deviation of values at the 3 plots is also shown. The data are divided into night and day, where night = 18.00-06.00 and day = 06.00-18.00. The data are obtained from the Bonanza Creek LTER website https://www.lter.uaf.edu/data/data-catalog. The grey bar shows the period of snowmelt at Eight Mile Lake catchment in May 2018.

Accepted Article

This article is protected by copyright. All rights reserved.

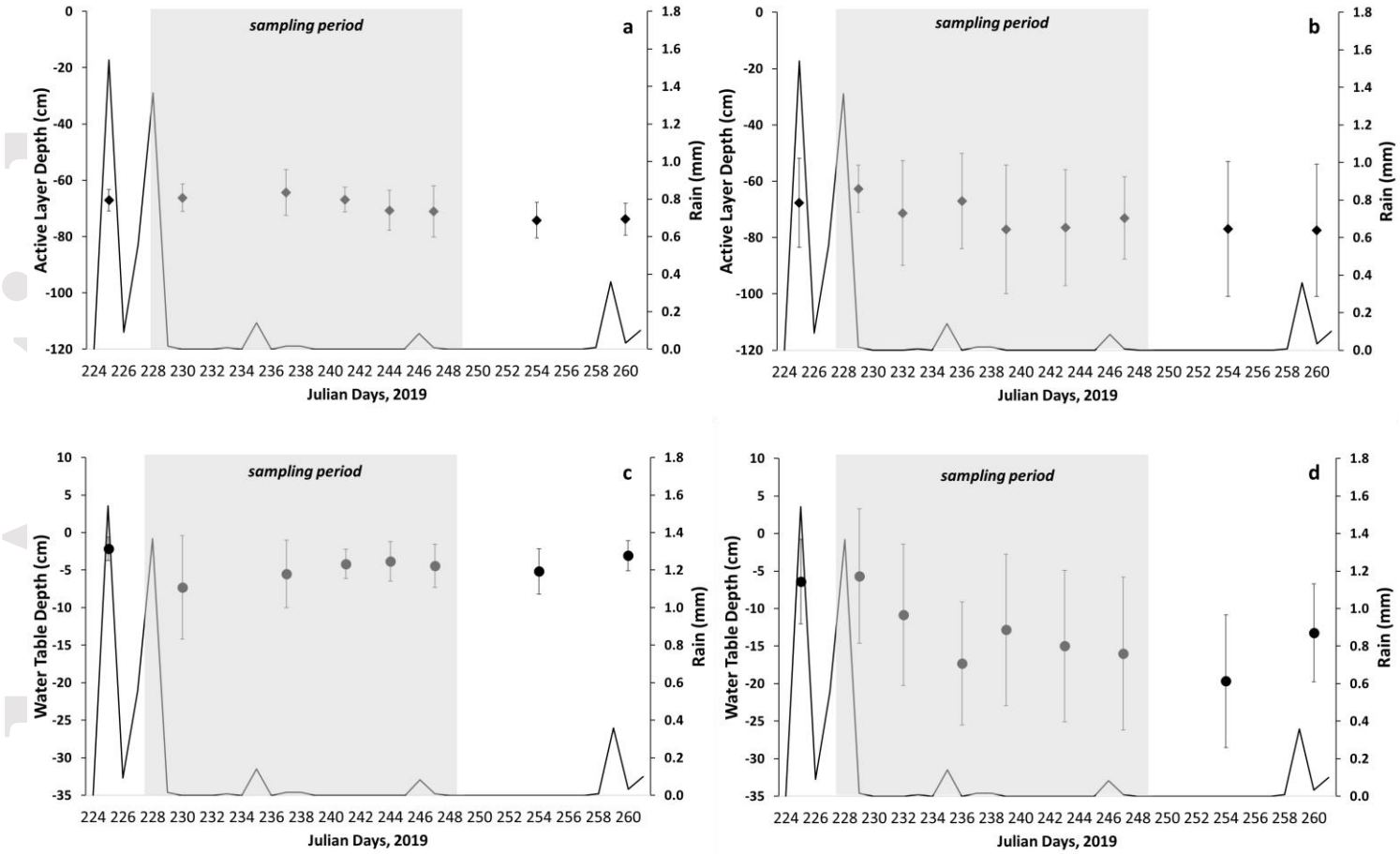


Figure S2. A time series of active layer depth (a and b) and water table depth (c and d) at sites of minimal (MIN) and extensive (EXT) permafrost degradation, between August 12 2019 (Julian Day = 228) and September 18 2019 (Julian Day = 261). Data show an average from six boreholes at MIN (plot 25-26, plot 27-28, plot 29-30, plot 31-32, plot 33-34, plot 35-36) and six boreholes at EXT (plot 1-2, plot 3-4, plot 5-6, plot 7-8, plot 9-10, plot 11-12). The standard deviation for the 6 boreholes at MIN and EXT is given. The hourly precipitation (mm) at Eight Mile Lake for this time period is also shown (https://www.lter.uaf.edu/data/data-catalog). The period of sampling (Julian Day 228 – 248) is shown in grey. The active layer depth and water table depth measured outside the sampling period are obtained from the Bonanza Creek LTER website https://www.lter.uaf.edu/data/data-catalog.

This article is protected by copyright. All rights reserved.

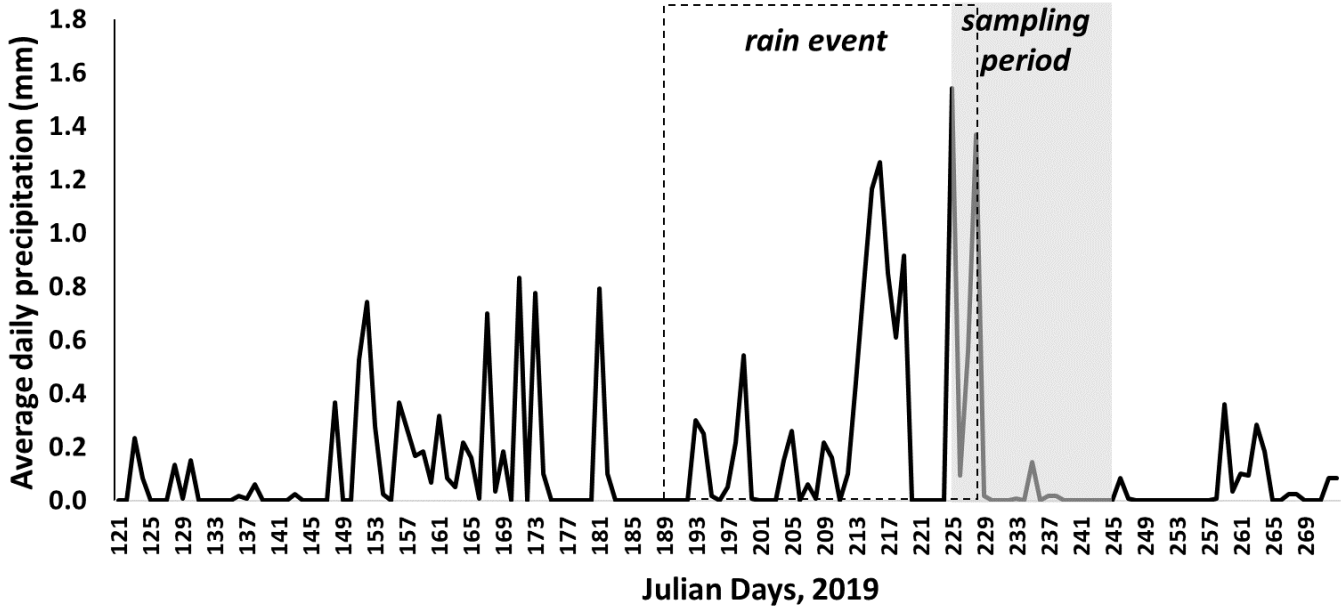


Figure S3. Hourly precipitation (mm) at Eight Mile Lake between May 1 2019 and September 30 2019 (as Julian days). The grey band highlights the rain event that occurred between July 12 and August 17 and the black dotted line shows the period of sampling at Eight Mile Lake and Panguingue Creek in 2019. The precipitation data are obtained from the Bonanza Creek LTER website https://www.lter.uaf.edu/data/data-catalog.

This article is protected by copyright. All rights reserved.

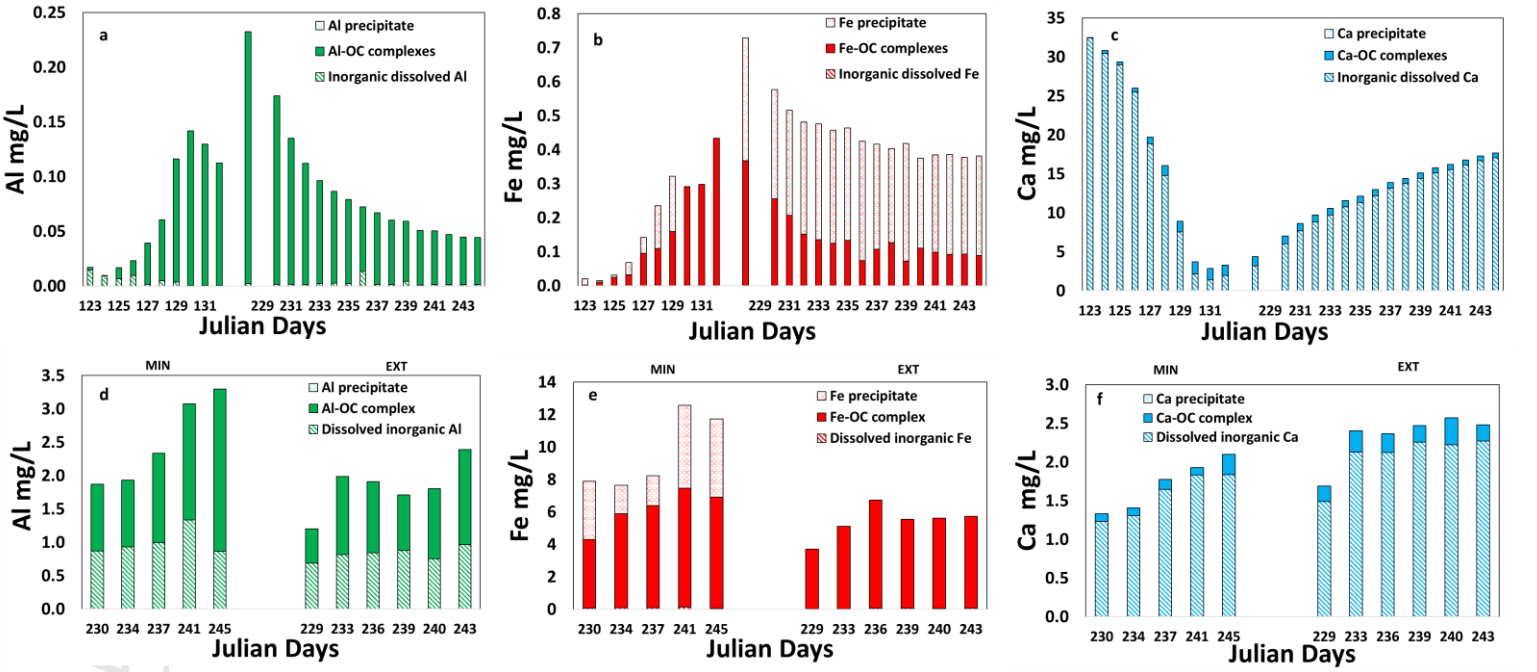


Figure S4. The proportion of Al (a), Fe (b) and Ca (c) transported as mineral precipitates, mineral element bound-dissolved organic carbon (DOC) and inorganic metal species in Panguingue Creek. Samples were collected daily between May 3 2018 and May 12 2018 and between August 16 2019 and September 2 2019. The proportion of Al (d), Fe (e) and Ca (f) transported as mineral precipitates, mineral element bound-dissolved organic carbon (DOC) and inorganic metal species in perched waters from sites of minimal (MIN) and extensive (EXT) permafrost degradation. Samples were collected between 17 August 2019 and 2 September 2019. The mineral element speciation was calculated using Visual MINTEQ version 3.2 (Gustafsson et al., 2011).

Accepted Article

This article is protected by copyright. All rights reserved.

Accepted Article

Parameter	*t statistic*	df	two-tailed p-value	Significant
Comparison between the 0-20 cm of soil at minimal and extensive sites in May 2018				
pH	7.19	22	0.0000	<0.01
conductivity	-2.65	22	0.0145	<0.05
DOC	-0.07	22	0.9421	no
Al	1.87	22	0.0750	<0.1
Fe	-2.41	22	0.0247	<0.05
Ca	-0.07	22	0.9420	no
Comparison between the unsaturated active layer at minimal and extensive sites in August 2019				
pH	1.36	15	0.1943	no
conductivity	-2.22	14	0.0436	<0.05
DOC	1.58	14	0.1373	no
Al	-0.57	15	0.5803	no
Fe	1.71	15	0.1079	no
Ca	-1.49	15	0.1572	no
Comparison between the saturated active layer at minimal and extensive sites in August 2019				
pH	-2.27	23	0.0330	<0.05
conductivity	-1.11	23	0.2801	no
DOC	4.81	22	0.0001	<0.001
Al	2.25	25	0.0337	<0.05
Fe	3.39	25	0.0023	< 0.005
Ca	0.01	25	0.9903	no
Comparison between the permafrost at minimal and extensive sites in August 2019				
pH	-1.75	14	0.1016	no
conductivity	-0.74	14	0.4715	no
DOC	2.09	14	0.0558	<0.1
Al	-0.58	14	0.5711	no
Fe	-1.24	14	0.2351	no
Ca	-1.87	14	0.0820	<0.1
Comparison between the perched waters at minimal and extensive sites in August 2019				
pH	-1.38	9	0.2023	no
conductivity	1.46	9	0.1773	no
DOC	0.32	9	0.7572	no
Al	-2.11	9	0.0643	<0.1
Fe	-4.02	9	0.0030	<0.01
Ca	3.15	9	0.0118	<0.05

This article is protected by copyright. All rights reserved.

Accepted Article

Parameter	*t statistic*	df	two-tailed p-value	Significant
Comparison between unsaturated active layer and saturated active layer at Minimal sites				
pH	-1.97	20	0.0626	no
conductivity	-0.51	19	0.6132	no
DOC	-3.37	20	0.0030	< 0.05
Al	-2.67	22	0.0139	< 0.05
Fe	-4.25	22	0.0003	< 0.001
Ca	-1.97	22	0.0620	no
Comparison between unsaturated active layer and saturated active layer at Extensive sites				
pH	-4.11	18	0.0007	<0.001
conductivity	0.42	18	0.6774	no
DOC	1.34	16	0.1992	no
Al	-0.11	18	0.9138	no
Fe	-1.24	18	0.2318	no
Ca	-1.52	18	0.1469	no
Comparison between saturated active layer and permafrost at Minimal sites				
pH	-4.87	21	0.0001	< 0.001
conductivity	-2.44	21	0.0238	< 0.05
DOC	-0.58	21	0.5696	no
Al	4.06	23	0.0005	<0.001
Fe	0.12	23	0.9036	no
Ca	-1.67	23	0.1090	no
Comparison between saturated active layer and permafrost at Extensive sites				
pH	-2.74	16	0.0144	<0.05
conductivity	-4.06	16	0.0009	<0.001
DOC	-2.47	15	0.0259	<0.05
Al	1.49	16	0.1550	no
Fe	-2.99	16	0.0086	<0.01
Ca	-4.21	16	0.0007	<0.001

Table S1. Welch t tests to differentiate between pH, conductivity, DOC, Al, Fe and Ca (i) in soil pore waters in the 0 – 20 cm of soil at MIN and EXT sites in May 2018; (ii) in soil pore waters in the unsaturated active layer in August 2019; (iii) in soil pore waters in the saturated active layer in August 2019, and (iii) in soil pore waters in the permafrost at MIN and EXT sites in August 2019; (iv) in the 0 – 30 cm of perched waters at MIN and EXT sites; (v) between the unsaturated active layer and saturated active layer at all MIN sites;

This article is protected by copyright. All rights reserved.

(vi) between the unsaturated active layer and saturated active layer at EXT sites; (vii) between the saturated active layer and permafrost at MIN sites and (viii) between the saturated active layer and permafrost at EXT site.

Accepted Article

This article is protected by copyright. All rights reserved.